Journal Pre-proof

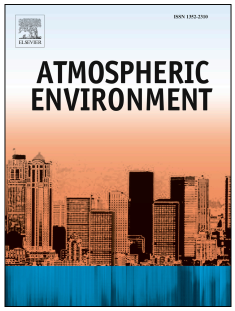

Classification of aerosols over Saudi Arabia from 2004–2016

Md Arfan Ali, Janet E. Nichol, Muhammad Bilal, Zhongfeng Qiu, Usman Mazhar, Md Wahiduzzaman, Mansour Almazroui, M. Nazrul Islam

PII: S1352-2310(20)30517-3

DOI: https://doi.org/10.1016/j.atmosenv.2020.117785

Reference: AEA 117785

To appear in: *Atmospheric Environment*

Received Date: 24 February 2020

Revised Date: 3 July 2020

Accepted Date: 12 July 2020

Please cite this article as: Ali, M.A., Nichol, J.E., Bilal, M., Qiu, Z., Mazhar, U., Wahiduzzaman, M., Almazroui, M., Islam, M.N., Classification of aerosols over Saudi Arabia from 2004–2016, *Atmospheric Environment* (2020), doi: https://doi.org/10.1016/j.atmosenv.2020.117785.

CRediT authorship contribution statement

Md. Arfan Ali: Conceptualization, Data curation, Methodology, Formal analysis, Investigation, Validation, Visualization, Writing - original draft. **Janet E. Nichol:** Supervision, Investigation, Writing - review & editing. **Muhammad Bilal:** Conceptualization, Investigation, Visualization, Writing - review & editing. **Zhongfeng Qiu:** Supervision, Writing - review & editing. **Usman Mazhar:** Data curation. **Md Wahiduzzaman:** Data curation. **Mansour Almazroui:** Data curation. **M. Nazrul Islam:** Data curation.

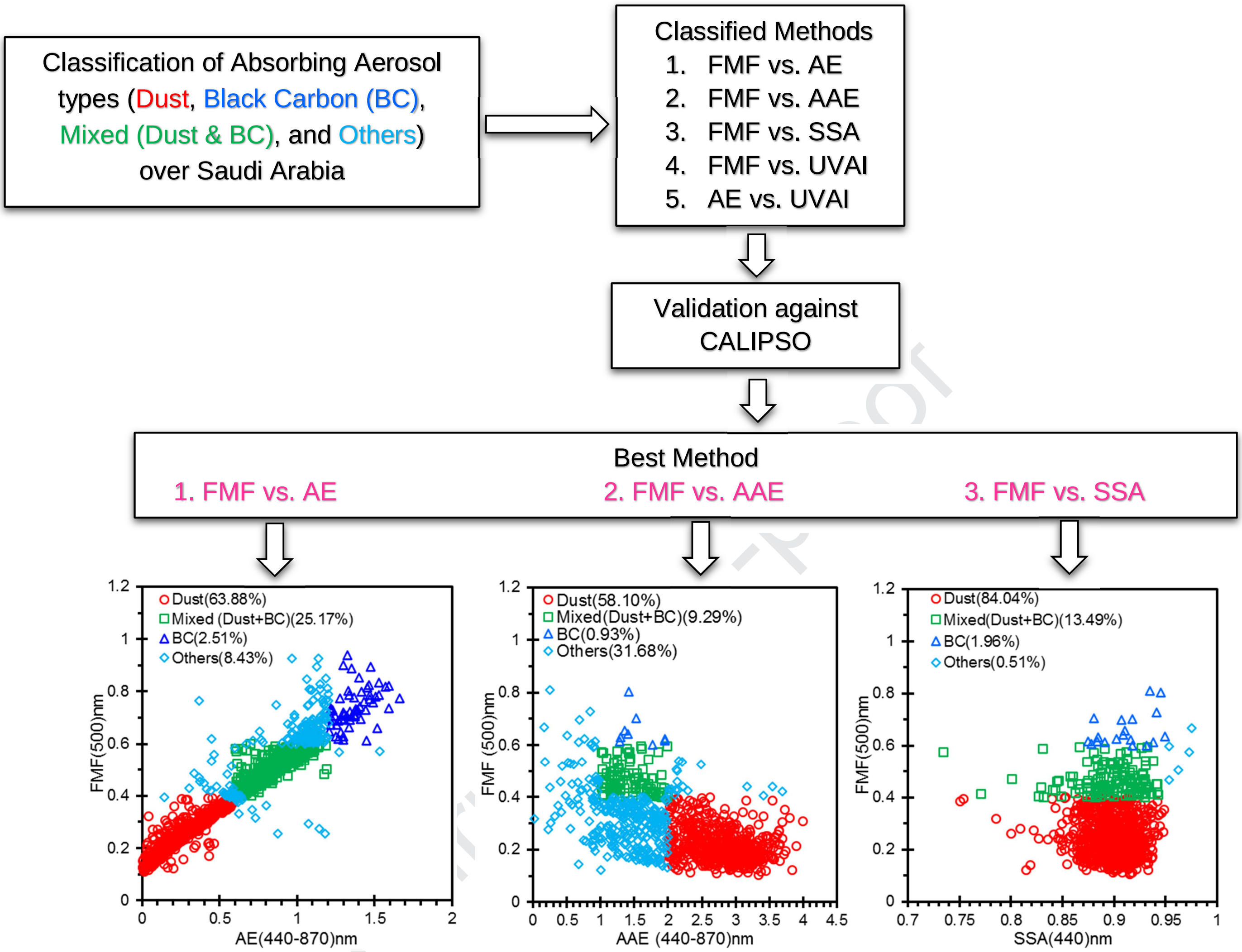
Classification of Absorbing Aerosol types (Dust, Black Carbon (BC), Mixed (Dust & BC), and Others) over Saudi Arabia
Classified Methods
1. FMF vs. AE
2. FMF vs. AAE
3. FMF vs. SSA
4. FMF vs. UVAI
5. AE vs. UVAI
Validation against CALIPSO
Best Method
1. FMF vs. AE
2. FMF vs. AAE
3. FMF vs. SSA
Dust(63.88%)
Mixed (Dust+BC)(25.17%)
BC(2.51%)
Others(8.43%)
FMF(500)nm
AE(440-870)nm
Dust(58.10%)
Mixed(Dust+BC)(9.29%)
BC(0.93%)
Others(31.68%)
FMF (500)nm
AAE (440-870)nm
Dust(84.04%)
Mixed(Dust+BC)(13.49%)
BC(1.96%)
Others(0.51%)
FMF(500)nm
SSA(440)nm

Classification of aerosols over Saudi Arabia from 2004−2016

Md. Arfan Ali[1, †], Janet E. Nichol[2, †], Muhammad Bilal[1*], Zhongfeng Qiu[1], Usman Mazhar[3], Md Wahiduzzaman[4], Mansour Almazroui[5], M. Nazrul Islam[5]

[1]School of Marine Sciences, Nanjing University of Information Science and Technology, Nanjing 210044, China

[2]Department of Geography, School of Global Studies, University of Sussex, UK

[3]School of Remote Sensing and Geomatics Engineering, Nanjing University of Information Science and Technology, Nanjing 210044, China

[4]Institute for Climate and Application Research, Nanjing University of Information Science and Technology, Nanjing 210044, China.

[5]Center of Excellence for Climate Change Research/Department of Meteorology, King Abdulaziz University, Jeddah 21589, Saudi Arabia

[*]Email: muhammad.bilal@connect.polyu.hk

†Authors with equal contributions.

Abstract

Knowledge of aerosol size and composition is very important for investigating the radiative forcing impacts of aerosols, distinguishing aerosol sources, and identifying harmful particulate types in air quality monitoring. The ability to identify aerosol type synoptically would greatly contribute to the knowledge of aerosol type distribution at both regional and global scales, especially where there are no data on chemical composition. In this study, aerosol classification techniques were based on aerosol optical properties from remotely-observed data from the Ozone Monitoring Instrument (OMI) and Aerosol Robotic Network (AERONET) over Saudi Arabia for the period 2004−2016 and validated using data from the Cloud-Aerosol Lidar and Infrared Pathfinder Satellite Observation (CALIPSO). For this purpose, the OMI-based

Aerosol Absorption Optical Depth (AAOD) and Ultra-Violet Aerosol Index (UVAI), and AERONET-based AAOD, Ångström Exponent (AE), Absorption Ångström Exponent (AAE), Fine Mode Fraction (FMF), and Single Scattering Albedo (SSA) were obtained. Spatial analysis of the satellite-based OMI-AAOD showed the dominance of absorbing aerosols over the study area, but with high seasonal variability. The study found significant underestimation by OMI AAOD suggesting that the OMAERUV product may need improvement over bright desert surfaces such as the study area. Aerosols were classified into (i) Dust, (ii) Black Carbon (BC), and (iii) Mixed (BC and Dust) based on the relationships technique, between the aerosol absorption properties (AAE, SSA, and UVAI) and size parameters (AE and FMF). Additionally, the AE vs. UVAI and FMF vs. UVAI relationships misclassified the aerosol types over the study area, and the FMF vs. AE, FMF vs. AAE and FMF vs. SSA relationships were found to be robust. As expected, the dust aerosol type was dominant both annually and seasonally due to frequent dust storm events. Also, fine particulates such as BC and Mixed (BC and Dust) were observed, likely due to industrial activities (cement, petrochemical, fertilizer), water desalination plants, and electric energy generation. This is the first study to classify aerosol types over Saudi Arabia using several different aerosol property relationships, as well as over more than one site, and using data over a much longer time-period than previous studies. This enables classification and recognition of specific aerosol types over the Arabian Peninsula and similar desert regions.

Keywords: Aerosols; AERONET; Single Scattering Albedo; Absorption Ångström Exponent; Ozone Monitoring Instrument; Aerosol Absorption Optical Depth.

1 Introduction

Atmospheric aerosol particles comprise solid and liquid materials differing in size from a few nanometers to larger than 100 micro-meters, with intricate composition and volatility in their physiochemical properties (Ali et al., 2019; Ali and Assiri, 2019; Almazroui, 2019). Over Asia, an immense diversity of aerosol types exist, due to rapid industrialization and urbanization. This creates uncertainty in assessing global climate change (Eck et al., 2010). Atmospheric aerosols are considered a major element of the earth’s climate system, as they remodel the climate and radiative balance directly by scattering and absorbing incoming solar radiation (Ali et al., 2017), whilst indirectly changing cloud optical properties and providing condensation nuclei (Kaufman et al., 2005). Classification of aerosols into different types can improve the precision of radiative balance, and assist climate modelling.

Aerosol types such as dust, organics, sea salt, and sulfate are predominantly reflective and scatter incoming solar radiation back to space, thus cooling the atmosphere (Bilal et al., 2013). However, other aerosols have more absorbing than scattering properties (Li et al., 2016). The main absorbers in the aerosol mixture are iron oxides from dust, and Black Carbon (BC) released from biomass burning and combustion processes and Brown Carbon (BrC) from organic mattter combustion (Wang et al., 2011). Moreover, iron oxides, BC and (BrC) show the greatest absorption from the ultraviolet (UV) to the visible region (Eck et al., 2010; Liakakou et al., 2020), while BC particles display constant absorption across the entire solar region (Bergstrom et al., 2002). A thorough understanding of climate forcing due to aerosol requires knowledge of aerosol concentration, its composition, size, and optical properties such as absorption or scattering. The aerosol size distribution and absorption properties can be used to classify the aerosols over the region (Higurashi and Nakajima, 2002; Lee et al., 2010). These properties vary spatially and temporally (Choi et al., 2009) according to the season, emission sources, and aerosol transportation (Ram et al., 2016).

The ground-based Aerosol Robotic Network (AERONET) provides aerosol absorptivity, from the Absorption Ångström Exponent (AAE) at 440–870 nm and Single Scattering Albedo (SSA) at 440 nm data. Complementing this, the Ozone Monitoring Instrument (OMI) on the Aura satellite also provides aerosol absorbing properties such as the Ultra-Violet Aerosol Index (UVAI) and Aerosol Absorption Optical Depth (AAOD) (Eq. 1) calculated in the UV and visible bands (Adesina et al., 2016) (Table 1). Light absorbing particles (e.g., dust, BC, or BrC) in the atmosphere can be determined by single scattering albedo (SSA) and absorbing aerosol optical depth (AAOD) (Shin et al., 2019). The AAOD is the columnar aerosol loading (i.e. AOD) due to light absorption based on the relationship

$$AAOD = (1-SSA) \times AOD \quad (1)$$

This is the most important parameter for the evaluation of atmospheric warming due to light absorbing aerosols. Hu et al. (2016) reported that high AAOD levels commonly found over East

Asia result mainly from aerosol mixtures comprising desert dust, industrial pollutants, and smoke from biomass burning. The study and classification of absorbing aerosols over the globe based on AERONET and satellite observations is well established (Cazorla et al., 2013; Logan et al., 2013; Logothetis et al., 2020; Kedia et al., 2014; Rupakheti et al., 2019, 2019a; Shen et al., 2019). Dubovik et al. (2002) established the relationship technique, which uses relationships between different optical properties of aerosols derived from AERONET and laboratory measurements, for the classification of global aerosols. Thus the relationship techniques of FMF (Fine Mode Fraction) vs. AE, FMF vs. AAE, FMF vs. SSA, AE vs. UVAI, and FMF vs. UVAI can be used to distinguish the major aerosol types (Tables 1 and 2). Since then, studies have used different relationship techniques, including FMF vs. AE (Eck et al., 2010), FMF vs. AAE (Giles et al., 2011), FMF vs. SSA (Lee et al., 2010; Giles et al., 2012), AE vs. UVAI and FMF vs. UVAI (Bibi et al., 2017) to classify aerosols into dust modes and BC). For example, low values of FMF vs. AE indicate coarse mode dust aerosol (Aloysius et al., 2009); and high values of FMF (> 0.6) and intermediate values of AAE (1.0 < AAE < 2.00) indicate BC aerosols (Giles et al., 2011). Similarly, values of SSA (SSA ≤ 0.95) and high values of FMF also indicate BC aerosols (Lee et al., 2010; Giles et al., 2012). Several studies have used relationship techniques from ground-based instruments alone, including Schmeisser et al. (2017), Jose et al. (2016) who classified absorbing aerosols over Hyderabad, India, Alam et al. (2016) over urban areas of Pakistan, and Gharibzadeh et al., (2018) over Iran. A validation and comparison of the classifications done based on FMF vs. SSA are suggested to be included with the previous studies done by Srivastava et al. (2012) and Tiwari et al. (2015) at different locations in India and Pakistan. Bibi et al. (2016; 2017) classified aerosol types using ground-based and satellite-based aerosol optical properties over Karachi (Pakistan) and the Indo-Gangetic Plain (IGP).

However, only a few such studies are available over the Middle-East. Of these, Farahat et al. (2016) reported only a single aerosol type: dust, over the Middle-East and North Africa. Al-Salihi (2018) classified aerosols based on AOD and AE relationship and over only one site, Baghdad, Iraq, reporting four different aerosol types (maritime, dust, urban, and biomass burning). The few aerosol classification studies conducted over Saudi Arabia have used only one site in Saudi Arabia, the Solar Village, as part of larger studies in other regions. For example, Logothetis et al. (2020) classified aerosols into eight types (Fine (highly, moderately, slightly, and non-absorbing), mixed (absorbing and non-absorbing), coarse (absorbing and non-absorbing)) based on FMF, SSA, and AE relationships over Europe, the Middle East, North-Africa and Arabian Peninsula. Kaskaoutis et al. (2007) classified aerosols into four types (clean maritime, biomass burning-urban, desert dust, and mixed) using relationship techniques over four continents and other studies include Chen et al. (2016) and Mao et al. (2019) who also included Saudi Arabia's Solar Village, Riyadh site as part of a larger study. None included the KAUST Campus site in Jeddah, which is situated at the other side of the country (Figure 1), and thus could offer a wider perspective of aerosol properties. Because Saudi Arabia has distinctive geographical and climatic environments, which differentiate it from other countries, accurate classification of aerosols cannot rely on universal classifications. High aerosol concentrations over Saudi Arabia have traditionally been attributed to frequent dust storms (Awad and Mashat, 2014; Almazroui et al., 2015; Awad et al., 2015; Kumar et al., 2018; Ali and Assiri, 2016, 2019; Mashat et al., 2019, 2020). However, the booming oil, and gas industry generating unprecedented economic growth, have stimulated, rapid urbanization and industrial

Table 1 Definition of aerosol optical properties and relationship indicators.

Index designation	**Name**	**Indicator**

AAOD	Aerosol Absorption Optical Depth	Columnar aerosol loading of light absorbing aerosols
AE	Ångström Exponent	Indicates the size of the dominant aerosol particles in the column (AE < 1 specifies dominance of coarse mode and AE > 1 demonstrates the dominance of fine mode aerosol)
AAE	Absorption Ångström Exponent	Measures the spectral dependence of absorption (UV to NIR), which depends on size, shape, and chemical composition of aerosols. Dust and BC (absorbing aerosols) have high values > 2.
FMF	Fine Mode Fraction	Provides quantitative information about the proportion of coarse and fine mode aerosol particles. FMF < 0.40 = coarse mode, 0.4 ≤ FMF ≥ 0.6 = mixture, FMF > 0.60 = fine mode
SSA	Single Scattering Albedo	The ratio of scattering to extinction, and indicates the proportion of absorbing versus scattering aerosol particles SSA > 0.95 = non-absorbing, SSA ≤ 0.95 = absorbing aerosols
UVAI	Ultra-Violet Aerosol Index	A robust index for detecting absorbing aerosols (dust and soot) in the atmosphere. Uses 2 UV wavebands. UVAI > 1.0 = the enhanced presence of UV-absorbing, UVAI = 0.5-1.0 = weak presence of UV-absorbing aerosols.
FMF vs. AE	Low values of both = Dust, Medium values = Mixed (BC and Dust), High values = BC	
FMF vs. AAE	High values of AAE and low values of FMF indicate Dust, Medium values of both indicate Mixed (BC and Dust), Low values of AAE and High values of FMF indicate BC	
FMF vs. SSA	Low values of FMF and Medium values of SSA indicate Dust, Medium values of FMF and Low SSA indicate Mixed (BC and Dust), and High values of both indicate BC.	
FMF vs. UVAI	Low values of FMF and High values of UVAI indicate Dust, Medium FMF and Low UVAI indicate Mixed (BC and Dust), High values of FMF and Low values of UVAI indicate BC	
AE vs. UVAI	Low values of AE and High values of UVAI indicate Dust, Medium AE, and Low UVAI indicate Mixed (BC and Dust), High values of AE, and Low values of UVAI indicate BC.	

activities (i.e., cement, petrochemical, fertilizer, water desalination, and electric energy generation plants). The outcomes are unquantified in terms of human health, as it is known that different aerosol types vary in their health impacts. Several studies have reported health impacts from heavy metals and pathogens accompanying dust storms over the Middle East. For example, Leili et al. (2008) examined total suspended particles and PM_{10} over the center of Tehran (Iran), and reported heavy metal contents (Pb, Co, Cd, Cu, and Cr) at levels dangerous enough to cause neurodevelopmental and behavioral defects in children. Other findings of high heavy metal content of airborne dust in the Middle East include Foroushani et al. (2019) in western Iran, and Farahmandkia et al. (2010) in Tehran. Studies, which linked heavy metals in dust with serious human health concerns, include Leili et al. (2008) in Tehran, Jiries et al. (2003) in Amman, Jordan, and Al-Rajhi et al. (1996) in Riyadh. In addition to heavy metals, Gerivani et al. (2011) found that dust storms in Iran can contain and transport viruses, which affect human populations and Saeedi et al. (2012) reported dust particles containing polycyclic aromatic hydrocarbons (PAHs) in Teheran. A potentially beneficial impact of dust particles, is their role in carrying nutrients to the marine ecosystem of the Northern Red Sea (Jeddah) and their contribution to nutrient balance continues largely unexplored (Prakash et al., 2015). The amplified threats of climate change for desert animals world-wide are magnified in Saudi Arabia (Williams et al., 2012). Thus, the classification of aerosols over the Arabian Peninsula for accurate estimates of climate forcing and health impacts is urgent. This study uses available ground-based AERONET sites within Saudi Arabia i.e., the Solar Village and KAUST Campus sites, combined with satellite data from the Ozone Monitoring Instrument (OMI) to classify the predominant types of aerosols over Saudi Arabia.

The main contributions of the current research are (a) the long-term period and spatial spread of observations that makes the results more robust and (b) the selection of the most appropriate technique (classification scheme) for the determination of different aerosol types over Arabia, based on comparison with CALIPSO.

2 Study area and Data-sets

2.1 Study Area

Saudi Arabia is the largest country in the Middle-East, covering 80% of the Arabian Peninsula with an area of approximately 2,218,000 km^2 (Figure 1), and is bordered by the Arabian Gulf and the Red Sea. The largest desert, the Rub al Khali or Empty Quarter covers 647,500 Km^2 in the southern part of the country and is a source of frequent dust outbreaks and severe dust storms. The country comprises 13 provinces and a total of 104 cities, of which the 20 largest have over 100,000 residents. This study was accomplished over the two AERONET ground stations in Saudi Arabia: Solar Village and KAUST Campus (Figure 1). The Solar Village (24.91˚ N, 46.41˚ E and 764 m a.s.l) is approximately 50 km from the north-west periphery of Riyadh. This city is situated on the desert plateau resulting in frequent dust storm events (Farahat, 2016). The KAUST Campus site (22.30˚ N, 39.10˚ E and 11.2 m a.s.l) is positioned in the village of Thuwal in a rural and coastal site in the Red Sea on the roof of a building. Climatically, the country has little rainfall, with approximately 100 mm between autumn and early spring, followed by hot and dry late spring and summer. The Shamal winds lead to dust events during spring (Mashat et al., 2020) and summer (Notaro et al., 2013, 2015; Yu et al., 2013, 2015, 2016), with over thus the KAUST Campus and Solar Village sites (Figure 1) observe higher aerosol loadings at these times.

Based on the three-month mean readings of temperature and rainfall, Saudi Arabia's seasons are classified into spring from March to May (MAM), summer from June to August (JJA), autumn from September to November (SON), and winter from December to February (DJF) (AMS, 2001).

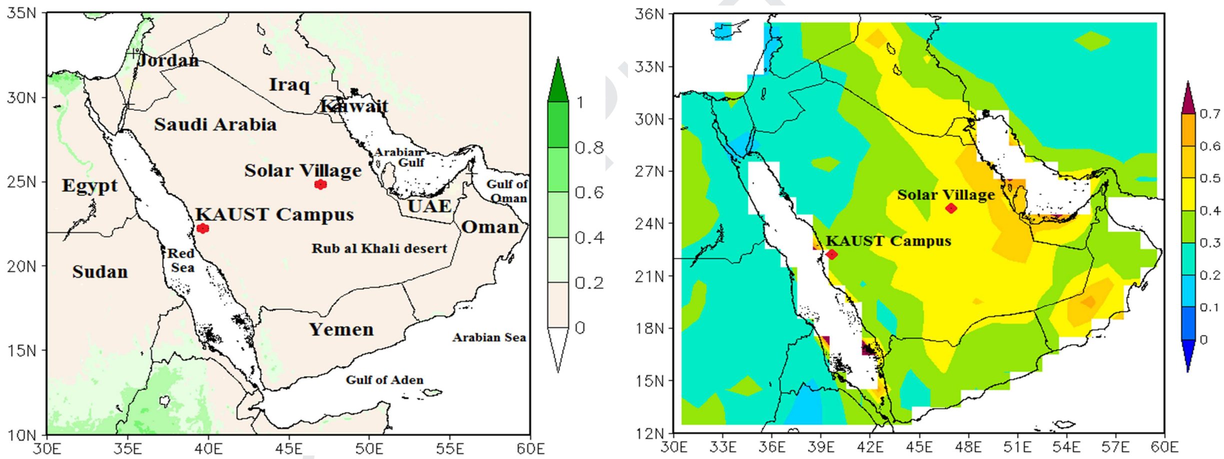

Figure 1: Geographical map of the Kingdom of Saudi Arabia. Red asterisks represent the two ground-based AERONET stations. Whereas, the left panel represents the mean values (2004–2016) of Normalized Difference Vegetation Index (NDVI) and the right panel represents the long-term (2004–2016) mean values of aerosol optical depth (AOD) based on the MODIS Collection 6.1 Deep Blue algorithm.

2.2 Data-sets

OMI is carried by the Aura satellite, launched in July 2004, and is designed to measure air quality, the earth’s climate, and ozone. It measures sunlight scattered by aerosols with high spectral resolution from the ultraviolet to visible regions (270−500 nm) and a spatial resolution of 13−24 km (Levelt et al., 2006). The OMI near-UV aerosol retrieval algorithm (OMAERUV) can be used to measure prominent absorbing aerosols such as dust and carbonaceous aerosols (Torres et al., 2007). The OMAERUV algorithm utilizes the near-UV spectral region for estimation of AAOD and UVAI products. Of major interest in the near-UV measurements is the powerful interaction between aerosol absorption and scattering in this spectral region, which facilitates the calculation of aerosol absorption capacity. For this study, OMI Level 2 and Level 3 OMAERUV OMI AAOD (500 nm) data were obtained from https://giovanni.gsfc.nasa.gov/mapss/ and "https://giovanni.gsfc.nasa.gov/giovanni/", respectively.

The Cloud-Aerosol Lidar and Infrared Pathfinder Satellite Observation (CALIPSO) was launched on 28th April 2006 on the CloudSat satellite to study the roles of aerosols and clouds in earth's air quality, weather and climate. The CALIPSO gives information on aerosol vertical profiles and 3-dimensional information of aerosol properties throughout day and night over the globe (Winker et al., 2003), based on the Cloud-Aerosol Lidar with Orthogonal Polarization (CALIOP) sensor. The aerosol lidar ratio, a key parameter for extinction retrieval, is determined for each aerosol subtype based on measurements, modelling, and the cluster analysis of a multiyear Aerosol Robotic Network (AERONET) dataset (Omar et al., 2005, 2009), they are considered more accurate than other measurements (Su et al., 2020). In version 3 (V3) and earlier, the CALIOP level 2 aerosol classification and lidar ratio selection algorithm defined six aerosol types: clean marine, dust, polluted continental, clean continental, polluted dust, and smoke (Omar et al., 2009). Each type is assigned an extinction-to-backscatter ratio (i.e., lidar ratio) with an associated uncertainty that defines the limits of its expected natural variability (https://www.atmos-meas-tech.net/11/6107/2018/amt-11-6107-2018.pdf). This study used the Level 2 CALIPSO version 4.10 aerosol-type profiles for aerosol classification. These images were downloaded from https://www-calipso.larc.nasa.gov/products/lidar/browse_images/std_v4_index.php. The temporal resolution of 16 days for CALIPSO makes it unsuitable for continuous monitoring, but due to its accuracy, it is used in this study for validation.

The AERONET is NASA's ground-based aerosol network, which has more than 700 stations over the globe (Holben et al., 1998). The data are commonly used for validating satellite-based aerosol retrievals. In this study, version-3 Level 2.0 (cloud-screened and quality-assured) daily averaged direct sun products (FMF_{440nm} and $AE_{440-870nm}$) and sky irradiance products ($AAOD_{440nm}$, SSA_{440nm}, and $AAE_{440-870nm}$) were obtained from https://aeronet.gsfc.nasa.gov/ for the period 2004–2016 (Table 2).

Table 2 Observation and the total number of datasets at each AERONET site.

Location	Observation	Total	
		Direct products AE/FMF	Inversion products SSA/AAE/AAOD
Solar Village	2004−May 2013	2463/2549	1001
KAUST Campus	Feb 2012−2016	1580/1393	1285

2.3 Research Methodology

The methodology of the present study is as follows: Mean seasonal and annual spatial distributions of OMI-AAOD were calculated from daily observations for the period 2004−2016. AERONET AAOD at 440 nm was interpolated to AAOD at 500 nm using the Ångström Exponent (Equation 1):

$$\mathrm{AAOD}_{500\ \mathrm{nm}} = \mathrm{AAOD}_{440\ \mathrm{nm}} \times \left(\frac{500}{440}\right)^{-\mathrm{AAE}_{440-870}} \qquad (2)$$

Monthly and seasonal temporal analyses were performed for the AERONET data (AAOD, AE, AAE, FMF, and SSA) and OMI data (AAOD and UVAI). For validation purposes, to obtain collocated OMI-AAOD with AERONET, the OMI AAOD values were averaged for a spatial window of 1×1 pixel centered over the Solar Village and KAUST Campus sites, and AERONET values were averaged for +/- 30mins of the overpass time of OMI. Similarly, OMI UVAI collocated retrievals were obtained which were used for the classification of aerosol types. In the present study, a total of five relationships such as FMF vs. AE (Logothetis et al., 2020), FMF vs. SSA (Logothetis et al., 2020; Lee et al., 2010), AE vs. UVAI and FMF vs. UVAI (Bibi et al., 2017) were used. Besides, the FMF vs. AAE relationship is modified based on several previously published studies (Lee et al., 2010; Bibi et al., 2017; Rupakheti et al., 2019; Logothetis et al., 2020). The above relationships classified aerosols into three main categories (Table 3), namely (1) dust, (2) mixed dust and black carbon (BC), and (3) BC (nearly exclusively attributed to fossil-fuel emissions, industrial and traffic). The remaining data points, which do not fall within the classification thresholds, are denoted as other aerosol types. Finally, the identified aerosol types were confirmed by comparison with satellite aerosol products from CALIPSO datasets.

Table 3 Classification of aerosol types over Saudi Arabia using threshold values taken from previous studies.

Aerosol Types	FMF vs AE		FMF vs AAE		FMF vs SSA	
Dust	FMF<0.4	AE<0.6	FMF<0.4	AAE>2.0	FMF<0.4	SSA≤0.95
Mixed (BC & Dust)	0.4≤FMF≤0.6	0.6≤AE≤1.2	0.4≤FMF≤0.6	1.0<AAE<2.0	0.4≤FMF≤0.6	SSA≤0.95
BC	FMF>0.6	AE> 1.2	FMF>0.6	1.0<AAE<2.0	FMF>0.6	SSA≤0.95

Aerosol Types	AE vs UVAI		FMF vs UVAI	
Dust	0.0<AE<0.4	UVAI>1.57	0.1<FMF<0.3	UVAI>1.57
Mixed (BC & Dust)	0.0<AE<1.0	0.5<UVAI<1.55	0.1<FMF<0.55	0.5<UVAI<1.55
BC	1.0<AE>1.55	0.5<UVAI<1.52	0.55<FMF>1.0	0.5<UVAI<1.50

3 Results and Discussion

3.1 Spatial distribution of OMI-based AAOD

Figures 2 and 3 show the mean annual and seasonal Level-3 OMI-AAOD retrievals at 500 nm of over Saudi Arabia for 2004−2016. Figure 2 shows high AAOD values (greater than 0.03) over the Eastern provinces, moderate AAOD (0.018 to 0.03) over most parts of the country, and low AAOD (0.01 to 0.018) in the North-Western region. These AAOD values are less than 10% of the columnar AOD values, which suggests that absorbing aerosols are much fewer than scattering aerosols over Saudi Arabia. High AAOD is mainly distributed near the sources of dust, BC, and OC (Islam et al., 2019; Kang et al., 2017). The seasonal distributions (Figure 3) show the highest AAOD (greater than 0.03) in spring, and over the Eastern and Southern provinces, followed by summer, winter, and autumn. This is because dust storms originate in the Sahara Desert due to depressions passing eastwards over the Mediterranean Sea, and strong ground heating produces turbulence, local pressure gradients, and the Shamal (wind) pattern (Shao, 2008; Prakash et al., 2015; Mashat et al., 2019). April to May (spring) experiences by peak dustiness over Eastern regions, and May-June over Southern and Central regions of Saudi Arabia (Sabbah and Hasan, 2008; Yu et al., 2013). However, an anticyclonic pattern is developed in autumn leading to weak dust activity resulting lowest columnar AAOD over Saudi Arabia (Kang et al., 2017; Mashat et al., 2019).

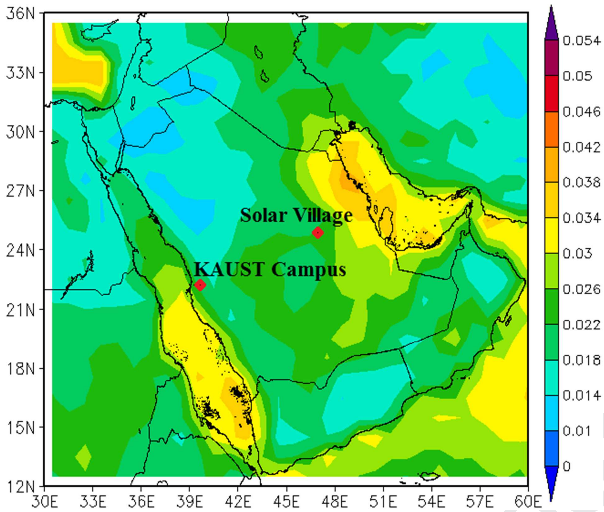

Figure 2: Annual mean Aerosol Absorption Optical Depth (AAOD) obtained from the OMI instrument over Saudi Arabia averaged over the period 2004−2016.

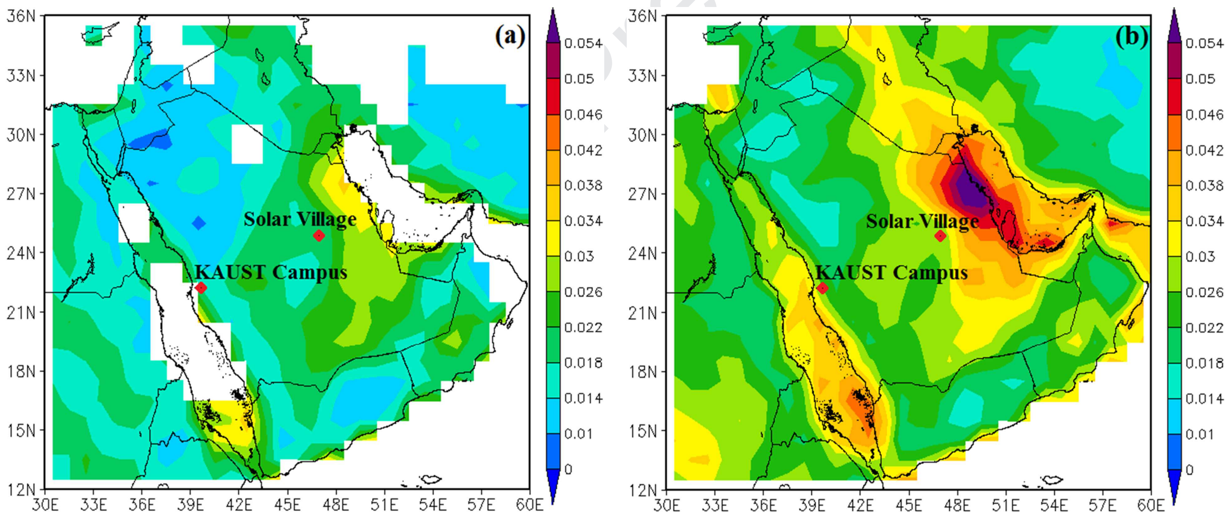

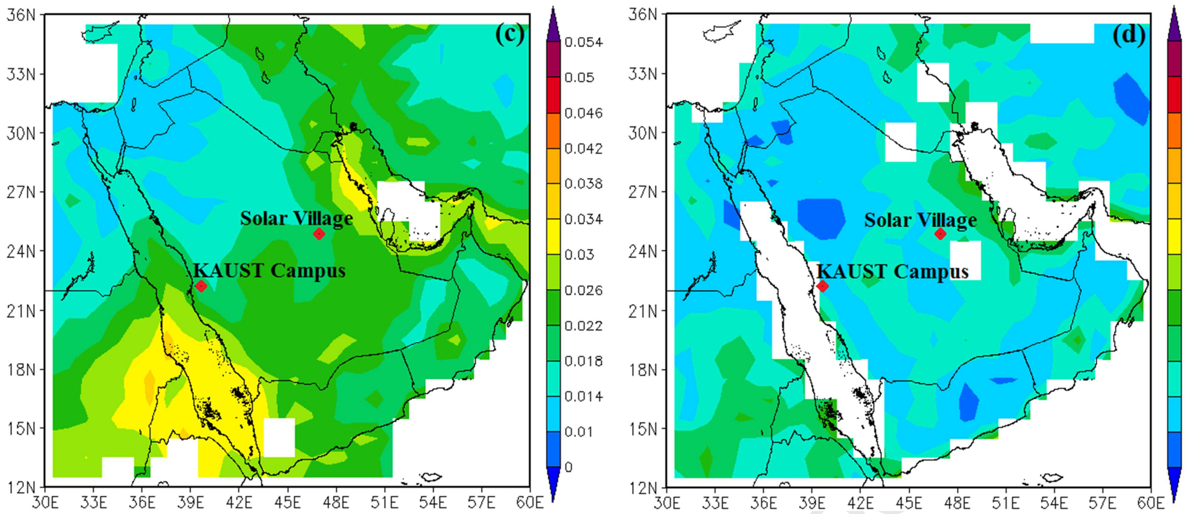

Figure 3: Mean seasonal spatial distribution of Aerosol Absorption Optical Depth (AAOD) for (a) Winter, (b) Spring, (c) Summer, and (d) Autumn obtained from OMI instrument over Saudi Arabia averaged over the period 2004−2016.

Figure 4 shows a more detailed annual cycle of both AERONET- and OMI-based Level-2 AAOD over the Solar Village (2004–2013) and KAUST Campus (2012–2016) sites. Higher values of AERONET and OMI AAOD retrievals over Solar Village in the east of the Peninsula indicate more absorbing aerosols present than over the KAUST Campus site. This may be due to a larger number of dust storm events compared to the KAUST region, as reported by Butt et al., 2017 using ground-based meteorological data. Results showed that OMI-AAOD retrievals followed the same temporal pattern as the AERONET-AAOD measurements (Figure 4). Figure 5 shows significant underestimations for both low and high aerosol loadings as indicated by lower values of the slope, which suggested the inappropriate use of the aerosol model as well as error in the estimated surface reflectance. The underestimation during the low aerosol loadings is caused by the overestimation in the estimated in the surface reflectance (Bilal et al., 2013; Bilal and Nichol, 2015). Error in these parameters might be responsible for the underestimation in the AAOD retrieved by the OMAERUV algorithm. This may suggest that improvements in the OMI algorithm (OMAERUV) are required for a better estimation of AAOD over bright desert surfaces.

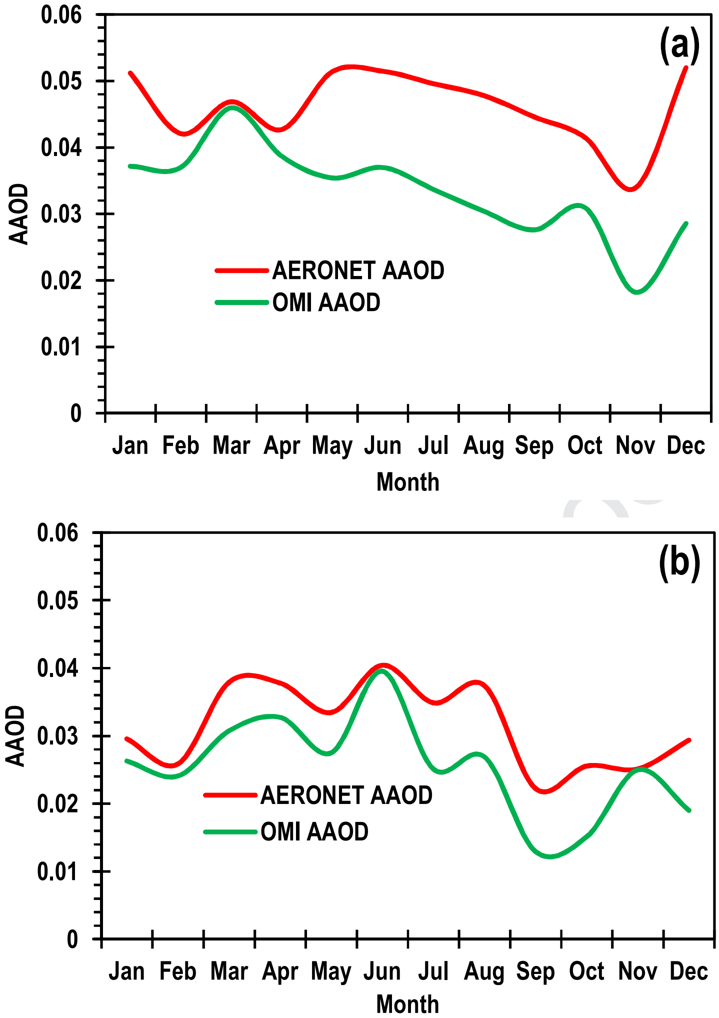

300 **Figure 4:** Annual cycle of Aerosol Absorption Optical Depth (AAOD) obtained from
301 AERONET and Level 2 OMI instrument over the (a) Solar Village (2004−2013) and (b) KAUST
302 Campus (2012−2016).

303

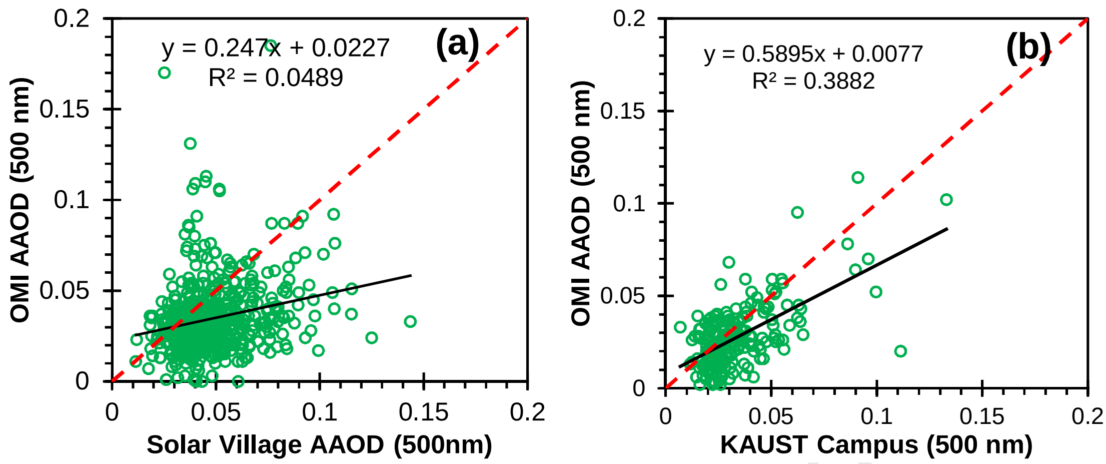

Figure 5: Scatterplot between OMI AAOD and AERONET AAOD over the (a) Solar Village (2004−2013) and (b) KAUST Campus (2012−2016).

Figure 6 represents the annual cycle of AERONET- and OMI-based aerosol optical properties over the Solar Village and KAUST Campus sites for the period 2004−2016. These properties describe both aerosol size and absorptivity, including Ångström Exponent (AE), Absorption Ångström Exponent (AAE), Fine Mode Fraction (FMF), Single Scattering Albedo (SSA), and Aerosol Index (UVAI). The AE indicates the size of the dominant aerosol particles in the column, where small values of AE (< 1) indicate the dominance of coarse mode aerosols and large values of AE (> 1) demonstrate the dominance of fine mode aerosol such as BC, sulfate, and organic carbon released from manmade activities (Eck et al., 1999). The annual values of AE (Table 4) suggest coarse mode aerosols over both AERONET sites (Solar Village: 0.48, KAUST Campus: 0.64), as well as in all seasons. AE reaches its minimum in May (Solar Village: 0.20, KAUST Campus: 0.35) and maximum in November (Solar Village: 0.86, KAUST Campus: 0.97) (Figure 6). These results suggest substantially more coarse mode aerosols in spring compared with other seasons. Trend analysis showed no significant increasing or decreasing trends in AE over either site (Table 4).

The Absorption Ångström Exponent (AAE) indicates the absorption contrast in relation to wavelength, which depends on particle size, shape, and chemical composition of the absorbing aerosols, which have a unique value (Russel et al., 2010; Li et al., 2016). For example, values of AAE < 2 and AAE > 2 indicate the fine mode and coarse mode absorbing aerosols respectively. Annual average values of AAE suggest coarse mode absorbing aerosols over both AERONET sites (Solar Village: 2.19, KAUST Campus: 2.27) (Table 4). However, significant variations were observed at monthly scales, with coarse mode absorbing aerosols observed in spring, but fine mode absorbing aerosols in winter over both sites (Figure 6). Overall, no significant decreasing/increasing trends in AAE were observed over either site (Table 4).

The Fine Mode Fraction (FMF) provides quantitative information about the proportion of coarse and fine mode aerosol particles, varying from 0 (coarse mode aerosols) to 1 (fine mode aerosols). According to Lee et al. (2010) and Logothetis et al. (2020), FMF < 0.40 represents coarse mode aerosols, 0.40 ≤ FMF ≤ 0.60 represents mixed type (coarse and fine mode) aerosols and FMF > 0.60 represents fine mode aerosols. The annual average value of FMF (0.34) in Solar Village is lower than that in KAUST Campus (0.40) and corresponds to more coarse mode aerosols over Solar Village. The seasonal average value of FMF (spring: 0.24, summer: 0.31, autumn: 0.44, winter: 0.38) in Solar Village is lower compared to that in KAUST Campus (spring: 0.30, summer: 0.37, autumn: 0.48, winter: 0.43), which suggest more coarse-mode aerosols over Solar Village (Table 4). Annual values of FMF were lower at SV than at KAUST Campus, due to lower levels in spring and early summer. These lower levels of FMF at Solar Village indicated more coarse mode aerosols, compared to mixed aerosols for these months at KAUST Campus. Therefore, overall annually, Solar Village experiences more coarse mode aerosols than KAUST Campus (Figure 6). Overall, no significant decreasing/increasing trends in FMF were observed over the years 2004−2016 (Table 4).

The Single Scattering Albedo (SSA) is the ratio of scattering to extinction and indicates the proportion of absorbing versus scattering aerosol particles. The value of SSA > 0.95 describes non-absorbing aerosols, 0.90 ≤ SSA ≤ 0.95 indicates weakly absorbing aerosols, 0.85 < SSA < 0.90 for moderately absorbing aerosols, and SSA < 0.85 belongs to highly absorbing aerosols (Lee et al., 2010; Russel et al., 2010; Gyawali et al., 2012; Shin et al., 2019). The annual average values of SSA within the range of 0.85−0.95 suggest the presence of weakly absorbing aerosols over both AERONET sites (Solar Village: 0.90, KAUST Campus: 0.93) (Table 4). At seasonal scale, weakly absorbing aerosols were observed during all seasons except during summer over the Solar Village site. Weakly absorbing aerosols indicate both dust and organic carbon, the latter being a complex mixture of chemical compounds generated from fossil fuel and biofuel burning as well as from natural biogenic emissions. The absorption or scattering property of dust grains depends on their size and composition, whether predominantly silicate or graphite, thus these results are compatible with the results of FMF and AE, which suggest coarse aerosols to be dominant at both sites. Overall, no significant decreasing/increasing trends in SSA were observed (Table 4).

The Ultra-Violet Aerosol Index (UVAI) is a well-known index for detecting the absorbing aerosols (dust and biomass burning) in the atmosphere. It uses the UV spectrum to distinguish absorbing from non-absorbing aerosols (Graaf et al., 2005). The threshold UVAI > 0.5 is useful to identify absorbing aerosols (Torres et al., 2009). The value of UVAI > 1.0 shows the enhanced presence of UV-absorbing aerosols (e.g., dust or smoke or biomass burning), and 0.5 < UVAI < 1.0 indicates the weak presence of UV-absorbing aerosols (Washington et al., 2003). The observed values of UVAI suggest the weak presence of UV-absorbing aerosols over both AERONET sites except in spring at Solar Village and summer at KAUST Campus (Table 4) and this is confirmed by the monthly values (Figure 6). These findings support Kaskaoutis et al. (2010) report of dust particles as indicated by the AI (0.5 to 0.6) over the South Greek sea regions. Overall, a significant increasing trend in UVAI was observed at KAUST Campus (Table 4).

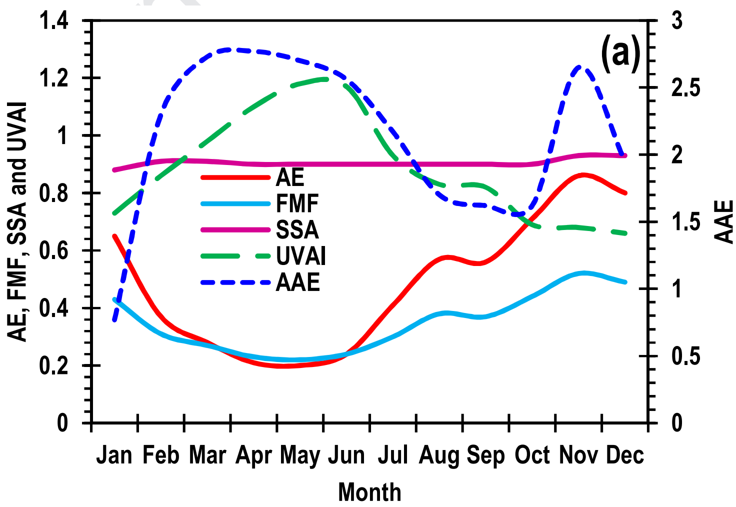

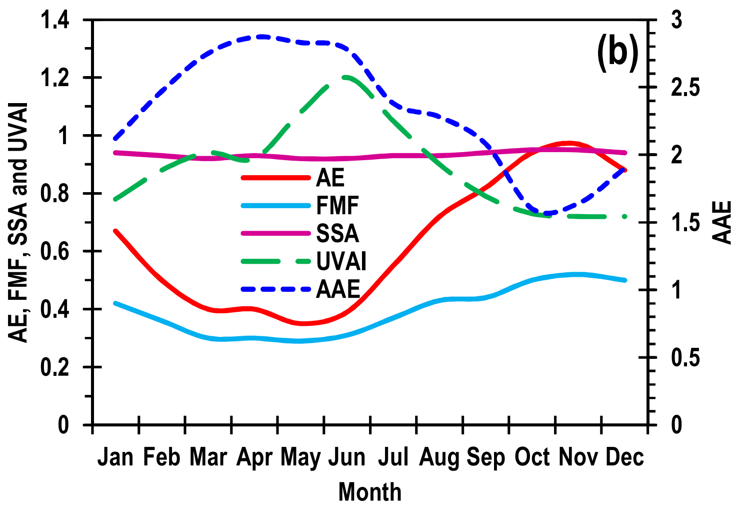

Figure 6: Annual cycle of averaged Aerosol Optical Properties obtained from AERONET (AE, AAE, FMF, and SSA), and OMI (UVAI) over the (a) Solar Village site (2004−2013) and (b) KAUST Campus site (2012−2016).

As can be seen from the above aerosol descriptions in this section 3.2, the analysis based on the individual parameters describe, whether fine or coarse mode (AE and FMF), whether fine or coarse mode absorbing aerosols (AAE), and whether absorbing or non-absorbing aerosols (SSA and UVAI). However, these individual parameters cannot identify the exact nature of the aerosol types such as dust or BC or mixed. Therefore, section 3.3 evaluates the combination of these parameters to classify aerosols into specific types.

Table 4 Mean seasonal and annual variability of aerosol optical properties (AE, AAE, FMF, SSA, and UVAI) with their trends over the Solar Village and KAUST Campus sites for the period 2004−2016.

Parameters	Solar Village						KAUST Campus					
	Winter	Spring	Summer	Autumn	Annual	Trends	Winter	Spring	Summer	Autumn	Annual	Trends
AE	0.54±0.17	0.23±0.12	0.41±0.17	0.70±0.18	0.48±0.25	-0.012	0.68±0.20	0.39±0.08	0.55±0.17	0.91±0.12	0.64±0.24	0.023
AAE	2.14±0.93	2.72±0.36	2.18±0.70	1.70±0.66	2.19±0.71	-0.044	2.19±0.40	2.80±0.28	2.48±0.48	1.77 ± 0.47	2.27±0.57	0.067
FMF	0.38±0.08	0.24±0.07	0.31±0.08	0.44±0.08	0.34±0.11	-0.008	0.43±0.07	0.30±0.04	0.37±0.07	0.48±0.05	0.40±0.09	0.007
SSA	0.900±0.03	0.902±0.01	0.897±0.01	0.903±0.20	0.90±0.02	-0.001	0.94±0.01	0.92±0.01	0.93±0.01	0.95±0.01	0.93±0.01	0.002
UVAI	0.78±0.17	1.09±0.20	0.97±0.20	0.73±0.12	0.88±0.23	0.012	0.79±0.15	0.98±0.20	1.05±0.24	0.75±0.11	0.89±0.22	0.015*

3.3 Classification of aerosols

The relationships of different parameters, namely FMF vs. AE, FMF vs. AAE, FMF vs. SSA, AE vs. UVAI, and FMF vs. UVAI were used to classify aerosols into three types: Dust, Mixed (Dust and BC), and BC (Figure 7–10). Results based on FMF vs. AE, FMF vs. AAE, and FMF vs. SSA demonstrated the dominance of Dust type aerosols followed by Mixed (BC and Dust), then BC over both sites, (Figures 7−10). Thus on Figures 7 and 8 (a–c), the relationships showing the dominance of Dust type aerosols were FMF vs. SSA (Solar Village: 84.04%%, KAUST Campus: 50.50%) followed by FMF vs. AE (Solar Village: 63.88%, KAUST Campus: 48.38%), and FMF vs. AAE (Solar Village: 58.10%, KAUST Campus: 46.45%). The results support observations of frequent dust storms (Kaskaoutis et al, 2007), as well as several studies reporting more dusty days over the Solar Village as compared to the KAUST Campus site (Yu et al., 2013; Butt et al., 2017), as many dust storms emanate from the desert of Iraq, North-East of Saudi Arabia, and Southern Iran, directly influencing to the Solar Village site (Prospero et al., 2003; Farahat et al., 2016). Therefore, dust aerosols are persistently prevalent over the Solar Village site. However, when we consider the relationships of AE vs. UVAI and

FMF vs. UVAI, these suggest the dominant aerosol type to be Mixed (BC and Dust) followed by Dust, and then BC (Figures 7 and 8 (d–e)). Since very low levels of Dust are indicated by the two relationships AE (Dust: 0.0<AE<0.4) vs. UVAI (Dust: >1.57) and FMF (Dust: 0.1<FMF<0.3) vs. UVAI (Dust: >1.57) over both sites, whereas the other three relationships show high dust levels, supported by the single parameters and by many other studies and reports, these results suggest that AE vs. UVAI and FMF vs. UVAI relationships cannot provide a meaningful aerosol types classification. This may be due to underestimation by the OMAERUV algorithm-based UVAI data (see Figures 4 and 5), as the UVAI alone suggested the dominance of absorbing aerosols over both sites. Therefore, the study indicates that the OMAERUV algorithm may need improvement for better estimating the OMI UVAI over bright-reflecting surfaces.

The value of FMF < 0.6 demonstrates coarse-mode dominated aerosols, which were associated with a mixture of different types of aerosols (Wu et al., 2015). Pérez-Ramírez et al., (2015), noted a similar finding over Granada, Spain. This interpretation is supported by Wu et al. 2015, who used a value of FMF < 0.6 to identify coarse-mode dominated aerosols which are associated with a mixture of different types of aerosols, and a similar finding was reported by Pérez-Ramírez et al., (2015) over Granada, Spain. The FMF (0.4 ≤ FMF ≤ 0.6) vs. AE (0.6 ≤ AE ≤ 1.2), FMF (0.4 ≤ FMF ≤ 0.6) vs. AAE (1.0 < AAE < 2.0), and FMF (0.4 ≤ FMF ≤ 0.6) vs. SSA (≤ 0.95) thresholds represent Mixed (Dust and BC) type aerosols. These Mixed type aerosols are best represented by FMF vs. AE (Solar Village: 25.17%, KAUST Campus: 41.21%), with the FMF vs. SSA and FMF vs. AAE giving lower percentages (Figures 7 and 8 (a–c)). Finally, Figures 7 and 8 (a–c) show a small percentages of BC aerosols based on the above-mentioned three relationships over the both sites. Higher FMF (> 0.6) values indicate fine mode aerosols, which correspond to BC, which may be due to local industrial activities (cement, petrochemical, and fertilizer), water desalination plants, and electric energy generation (Farahat et al., 2016). Some aerosol types were not classified namely ’Other’ type (Figures 7–10). These were best represented by FMF vs. AE (31.68%) over the Solar Village and by FMF vs. AAE (29.97%) over the KAUST Campus site (Figures 7 and 8 (a–c). These aerosols may be formed due to the mixing of natural and anthropogenic aerosols atmospheric water vapor over the study area (Kaskaoutis et al., 2011).

The seasonal distribution of aerosol types from the three relationships FMF vs. AE, FMF vs. AAE, and FMF vs. SSA confirm that Dust is the dominant aerosol type during all seasons over both sites, and this reaches its maximum in spring followed by summer, winter, and autumn (Figures 9 and 10 (a–c)). This confirms the findings of previous satellite- and station-based studies which reported high dust levels during the peak dust storm season of spring and early summer (Sabbah and Hasan, 2008; Yu et al., 2013; Farahat et al., 2016; Albugami et al., 2019). Conversely, the lowest FMF values (< 0.3) were noted in spring and summer over both sites, which support the findings of Kaskaoutis et al. (2007) and Wu et al. (2015). The above-mentioned three relationships indicate Mixed (Dust and BC) type aerosols during all seasons, with highest levels in autumn followed by winter, summer, and spring (Figures 9 and 10 (a–c)). The possible reasons for this decline in dust storm events as well as washing out by the higher rainfall during autumn to winter (Kaskaoutis et al., 2007; Farahat et al., 2016), resulting in FMF values become a little higher varies from 0.46 to 0.50 indicate coarse-mode dominated aerosols (Dust), which correspond to Mixed (Dust and BC) over the study area. The value of FMF < 0.6 demonstrates coarse-mode dominated aerosols, which were associated with a mixture of different types of aerosols (Lee et al., 2010; Wu et al., 2015). Figures 9 and 10 also show BC aerosols to be dominant during autumn and winter, which is attributed to local anthropogenic activities of urban/industrial and biofuel emission. Consequently, the FMF values are increased to above 0.6, and this is correlated with the observed fine-mode BC particles over the study area. These findings also supported by Gautam et al. (2007), Wu et al. (2015), and Lee et al. (2010).

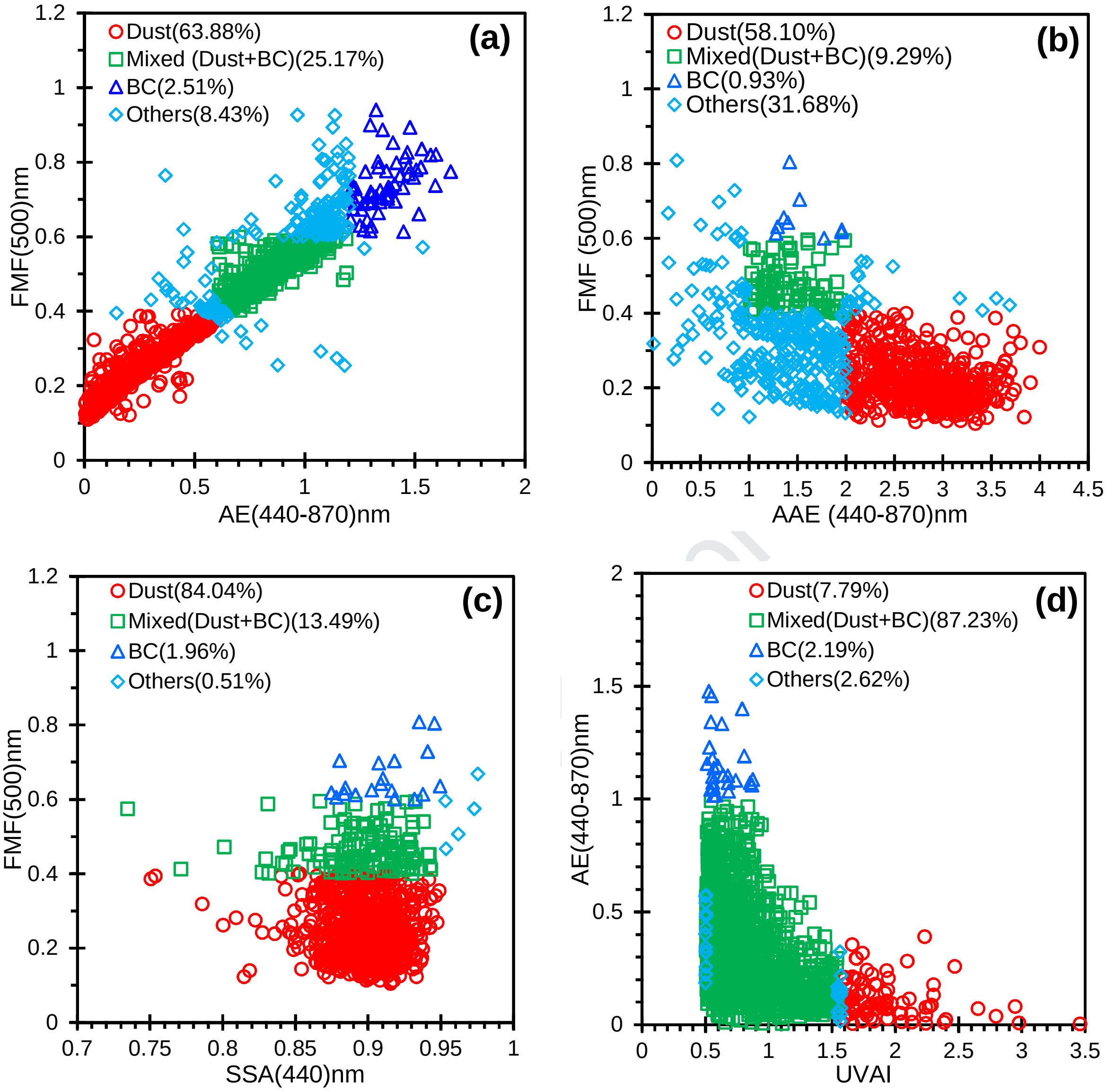
(a)
Dust(63.88%)
Mixed (Dust+BC)(25.17%)
BC(2.51%)
Others(8.43%)
FMF(500)nm
AE(440-870)nm
(b)
Dust(58.10%)
Mixed(Dust+BC)(9.29%)
BC(0.93%)
Others(31.68%)
FMF (500)nm
AAE (440-870)nm
(c)
Dust(84.04%)
Mixed(Dust+BC)(13.49%)
BC(1.96%)
Others(0.51%)
FMF(500)nm
SSA(440)nm
(d)
Dust(7.79%)
Mixed(Dust+BC)(87.23%)
BC(2.19%)
Others(2.62%)
AE(440-870)nm
UVAI

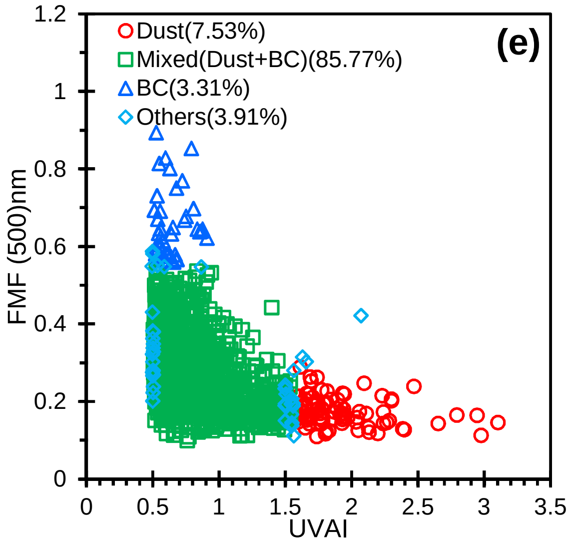

Figure 7: Aerosol classification over the Solar Village site during the period 2004-2013 for (a) FMF vs. AE, (b) FMF vs. AAE, (c) FMF vs. SSA, (d) AE vs. UVAI, and (e) FMF vs. UVAI.

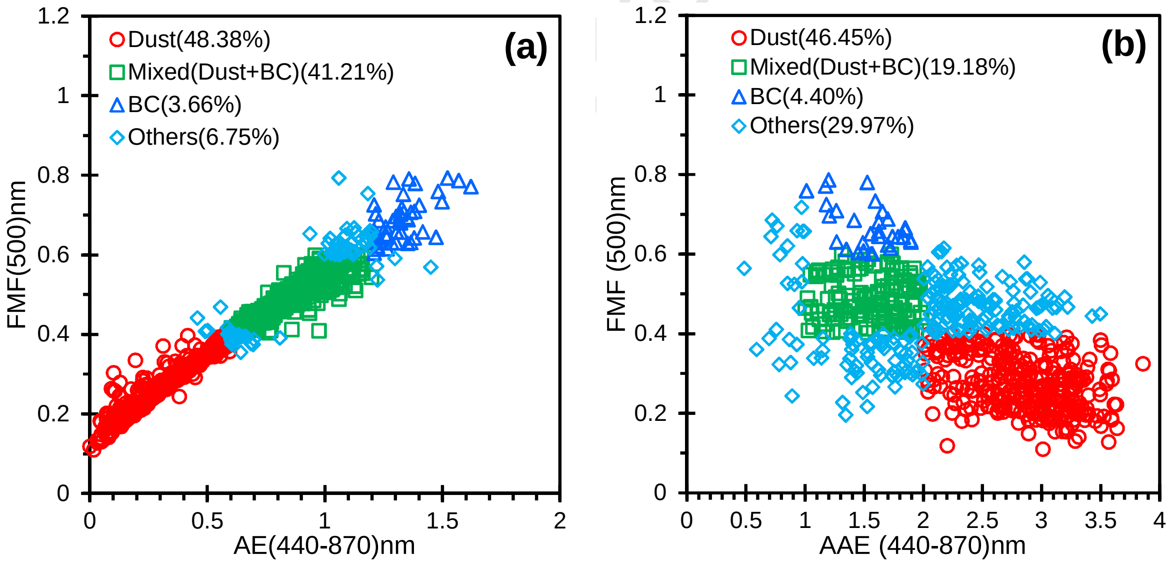

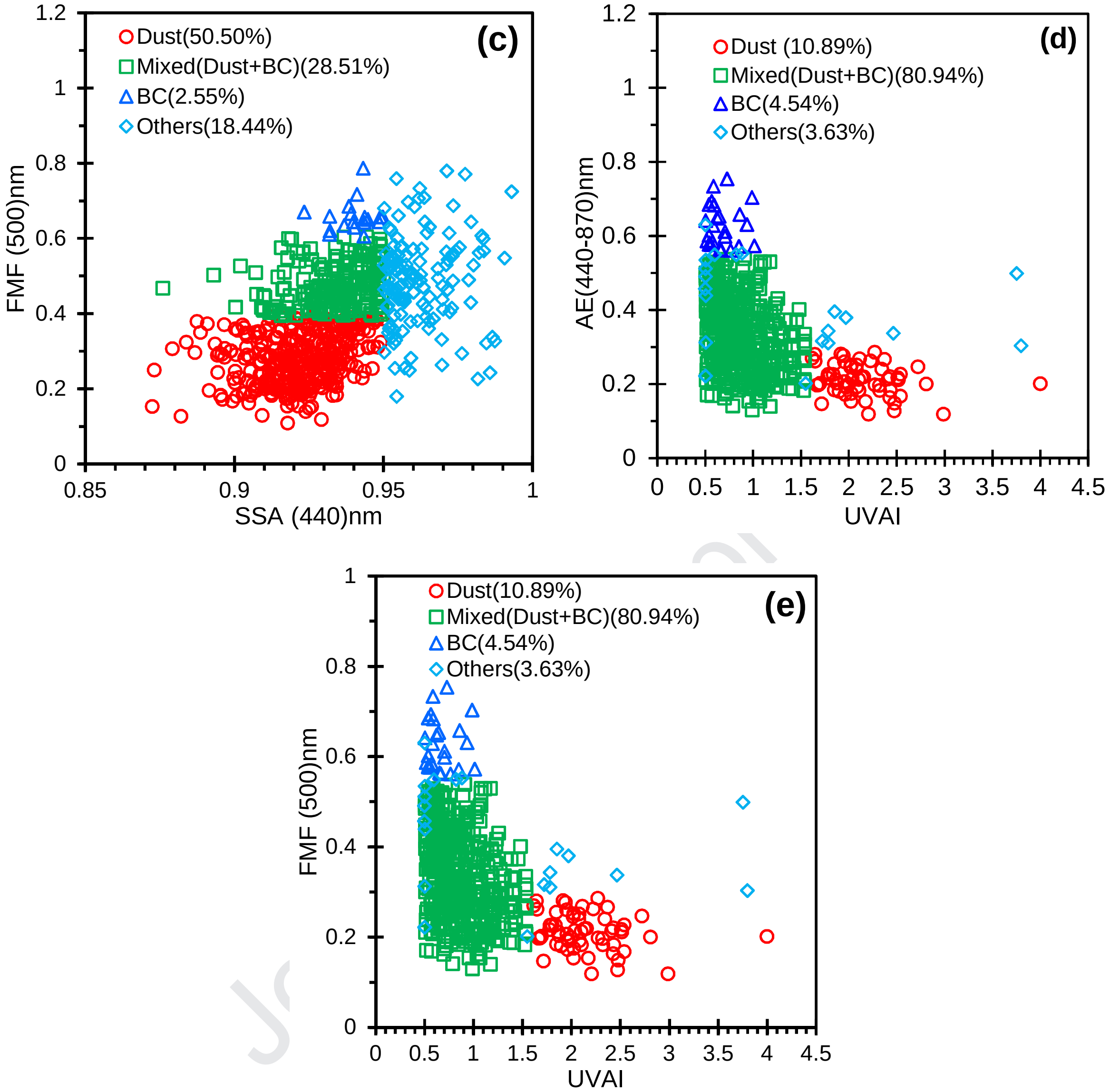

Figure 8: Aerosol classification over KAUST Campus site during the period 2012-2016 for (a) FMF vs. AE, (b) FMF vs. AAE, (c) FMF vs. SSA, (d) AE vs. UVAI, and (e) FMF vs. UVAI.

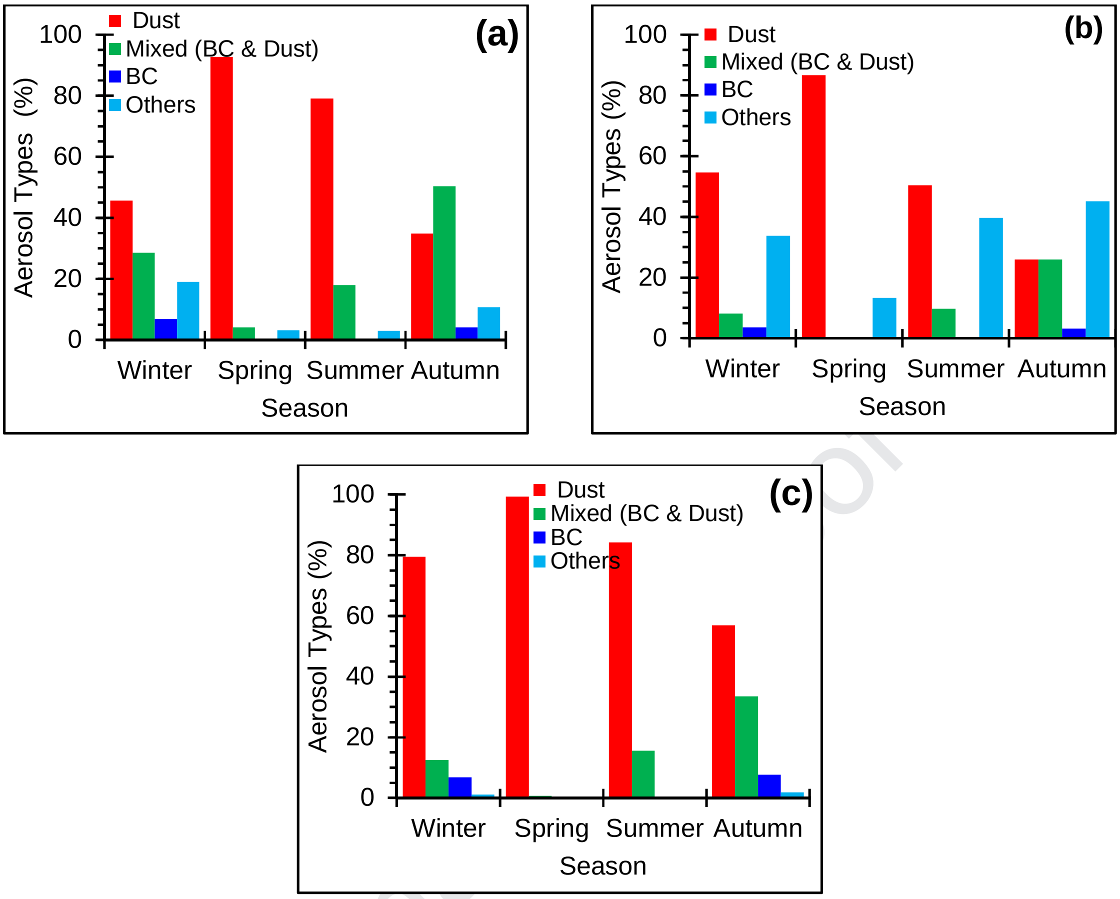

Figure 9: Seasonal aerosols classification over the Solar Village site during the period 2004-2013 for (a) FMF vs. AE, (b) FMF vs. AAE, (c) FMF vs. SSA.

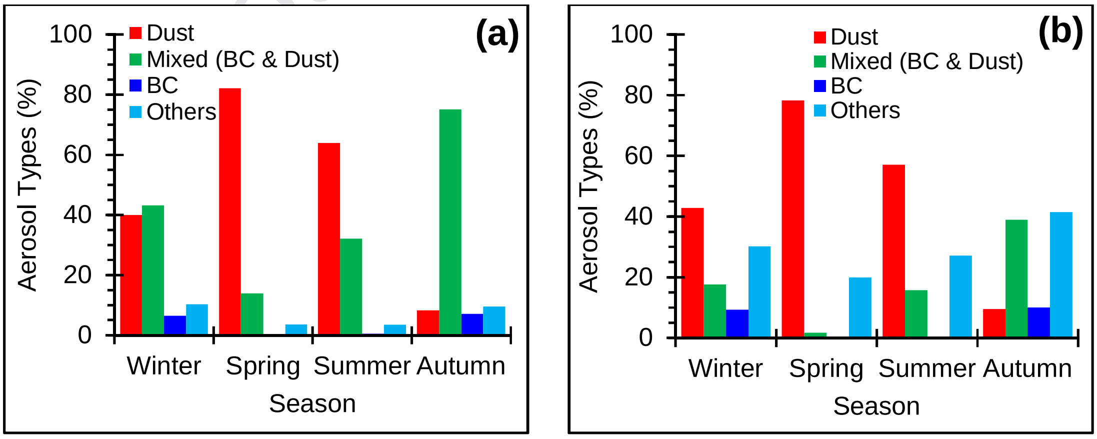

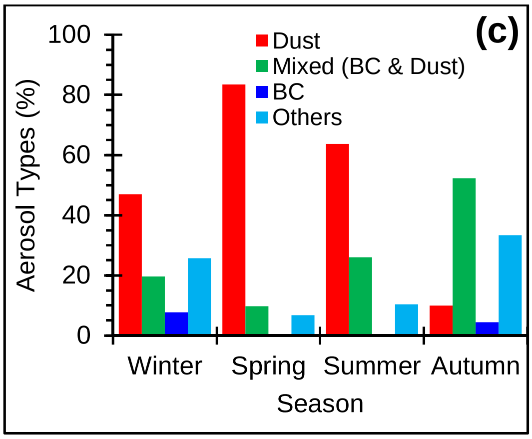

Figure 10: Seasonal aerosols classification over KAUST Campus site, Saudi Arabia during the period 2012–2016 for (a) FMF vs. AE, (b) FMF vs. AAE, (c) FMF vs. SSA.

3.4 Validation of Classified Aerosol Types

Classified aerosol types were validated against CALIPSO daytime aerosol type profiles. A similar approach was used in previous studies (Bibi et al., 2016, Bibi et al., 2017; Rupakheti et al., 2019), as no other data are available for validation. The CALIPSO (daytime) aerosol type profiles were downloaded for specific dates, according to the availability of AERONET data, including 24-Jul-2007, 11-Jul-2010, 06-Mar-2011, 29-Mar-2011, and 21-Apr-2008 for the Solar Village site, and 23-May-2012, 25-Jan-2013, 10-Feb-2013, 5-Mar-2013, and 02-Jun-2013 for the KAUST Campus site. Results from CALIPSO showed the dominance of Dust aerosol types reaching up to 5 km from the surface over both sites (Table 5 and Figures S1–S2). Results also showed the presence of other mixed aerosols (i.e. dust plumes and biomass burning mixed and forming polluted dust) over the study area (Table 5 and Figure S2–S3). The results showed a good agreement between FMF vs. AE, FMF vs. AAE, and FMF vs. SSA and the CALIPSO classified aerosol types over the region. Therefore, this study recommends use of these three relationship techniques for aerosol classification over Saudi Arabia and other regions with similar atmospheric and land surface characteristics.

Table 5 Aerosol classifications based on FMF vs. (AE, AAE, and SSA) and CALIPSO.

Date	FMF vs. AE		Types	FMF vs. AAE		Types	FMF vs. SSA		Types	CALIPSO
Site: Solar Village										
24-Jul-2007	0.24	0.26	Dust	0.24	2.43	Dust	0.24	0.89	Dust	Dust
21-Apr-2008	0.15	0.04	Dust	0.15	3.23	Dust	0.15	0.92	Dust	Dust
11-Jul-2010	0.32	0.46	Dust	0.32	2.70	Dust	0.32	0.93	Dust	Dust

06-Mar-2011	0.25	0.36	Dust	0.25	3.45	Dust	0.25	0.88	Dust	Dust
29-Mar-2011	0.13	0.01	Dust	0.13	2.92	Dust	0.13	0.92	Dust	Dust
Site: KAUST Campus										
23-May-2012	0.29	0.23	Dust	0.29	2.89	Dust	0.29	0.90	Dust	Dust
25-Jan-2013	0.48	0.91	Mixed	0.48	1.41	Mixed	0.48	0.93	Mixed	Mixed
10-Feb-2013	0.37	0.55	Dust	0.37	2.01	Dust	0.37	0.93	Dust	Dust
5-Mar-2013	0.37	0.56	Dust	0.37	2.49	Dust	0.37	0.94	Dust	Dust
02-Jun-2013	0.19	0.10	Dust	0.19	3.15	Dust	0.19	0.90	Dust	Dust

4. Conclusion

In this paper, aerosol types over Saudi Arabia were classified using the aerosol property relationships technique and data from OMI (AAOD, UVAI) and AERONET (AAOD, AE, AAE, FMF, SSA). Based on the three relationships FMF vs. AE, FMF vs. AAE, and FMF vs. SSA, the study found dust to be the most common and abundant aerosol type at both annual and seasonal scales, and this was expected, due to the frequent dust storm activity over the study area. Notable temporal variations in aerosol type were observed and attributed to seasonal climatic changes, especially the greater percentage of Dust aerosol types in spring due to depressions passing eastwards over the Sahara Desert, a major dust source. Local dust sources are also more significant during the hot and dry seasons of spring to early summer; spatial variations are also significant, with high AAOD values over the Eastern and Southern provinces, due mainly to local dust sources, and lower AAOD over the Northern Province. Besides Dust, significant amounts of BC and Mixed (Dust and BC) aerosols were observed, though in lesser amounts than Dust, which are attributed to increasing industrial activities (cement, petrochemicals and fertilizers), water desalination plants, infrastructure, and electric energy generation. These release absorbing and fine particles, which often become mixed with dust. Significant underestimation in OMI UVAI and AAOD products was observed, suggesting that significant improvements are required for the OMI OMAERUV algorithm for better estimation of AAOD over bright desert surfaces. Consequently the study found that the relationships FMF vs. UVAI and AE vs. UVAI (with UVAI derived from OMI) relationships misclassified aerosol types over the study area, therefore the relationships FMF vs. AE, FMF vs. AAE, and FMF vs. SSA are recommended for aerosol classification over Saudi Arabia and areas with similar land and atmospheric characteristics. Validation of the classified aerosol types against CALIPSO data showed that the recommended aerosol classifiation relationships (FMF vs. AE, FMF vs. AAE, and FMF vs. SSA) are robust and effective for aerosol classsification over Saudi Arabia. In view of increased knowledge of the harmful health effects of dust-borne synthetic compounds, the aerosol relationships for identifying the specific aerosol types described here, should be of benefit in future air quality control programs, as well as in global studies of climatic forcing due to aerosol in arid regions.

Acknowledgment

The authors are grateful to the NASA Goddard Space Flight Center and Goddard Earth Sciences Data and Information Services Center (GESDISC) for providing OMI (UVAI and AAOD) and AERONET data. We would like to give special thanks to the scientific teams of CALIPSO for making the data available for this study. This research is supported by the Special Project of Jiangsu Distinguished Professor (1421061801003 and 1421061901001), the National Natural Science Foundation of China (Grant No. 41976165), and the Startup Foundation for Introduction Talent of NUIST (2017r107). The foremost author (Md. Arfan Ali) is highly grateful to the China Scholarship Council (CSC) and NUIST to grant the fellowship and providing the required supports.

References

Adesina, J.A., Kumar, K.R., Sivakumar, V., Piketh, S.J., 2016. Intercomparison and assessment of long-term (2004−2013) multiple satellite aerosol products over two contrasting sites in South Africa. J. Atmos. Sol. Terr. Phys. 148, 82−95.

Alam, K., Shaheen, K., Blaschke, T., Chishtie, F., Khan, H.U., Haq, B.S., 2016. Classification of Aerosols in an Urban Environment on the Basis of Optical Measurements. Aerosol and Air Quality Research, 16: 2535–2549.

Albugami, S., Palmer, S., Cinnamon, J., Meersmans, J., 2019. Spatial and Temporal Variations in the Incidence of Dust Storms in Saudi Arabia Revealed from In Situ Observations. Geosciences 9, 162; doi: 10.3390/geosciences9040162.

Ali, M.A., Assiri, M.E., 2016. Spatio-temporal analysis of aerosol con-centration over Saudi Arabia using satellite remote sensing tech-niques. Malays J Soc Sp 12:1–11.

Ali, M.A., Assiri, M.E., 2019. Analysis of AOD from MODIS- Merged DT–DB Products over the Arabian Peninsula. Earth Syst Environ 3, 625–636.

Ali, M.A., Assiri, M., Dambul, R., 2017. Seasonal Aerosol Optical Depth (AOD) variability using satellite data and its comparison over Saudi Arabia for the period 2002–2013. Aerosol Air Qual. Res. 17, 1267–1280.

Ali, M.A., Islam, M.M., Islam, M.N., Almazroui, M., 2019. Investigations of MODIS AOD and cloud properties with CERES sensor based net cloud radiative effect and a NOAA HYSPLIT Model over Bangladesh for the period 2001–2016. Atmos. Res. 215, 268−283.

Almazroui, M., 2019. A comparison study between AOD data from MODIS deep blue collections 51 and 06 and from AERONET over Saudi Arabia. Atmos. Res. 225, 88−95.

Almazroui, M., Dambul, R., Islam, M.N., Jones, P.D., 2015. Atmospheric circulation patterns in the Arab region and its relationships with Saudi Arabian surface climate: a preliminary assessment. Atmos. Res. 161–162, 36–51.

Aloysius, M., Mohan, M., Suresh Babu, S., Parameswaran, K., Moorthy, K.K., 2009. Validation of MODIS derived aerosol optical depth and an investigation on aerosol transport over the South East Arabian sea during ARMEX-II. Ann. Geophys. 27, 2285−2296.

AMS, 2001. Statement on seasonal to inter-annual climate prediction. Bull. Am. Meteorol. Soc. 82, 701–703.

Al-Rajhi, M.A., Seaward, M.R.D., Al-Aamer, A.S., 1996. Metal levels in indoor and outdoor dust in Riyadh, Saudi Arabi. Environment International, 22, 315-324.

Al-Salihi, A.M., 2018. Characterization of aerosol type based on aerosol optical properties over Baghdad, Iraq. Arab. J. Geosci. 11, 633.

Awad, A., Mashat, A., 2014. The synoptic patterns associated with spring widespread dusty days in central and eastern Saudi Arabia. Atmosphere 5 (4), 889–913.

Awad, A.M., Mashat, A.S., Salem, F.F.A., 2015. Diagnostic study of spring dusty days over the southwest region of the Kingdom of Saudi Arabia. Arab. J. Geosci. 8, 2265–2282.

Bergstrom, R.W., Russell, P.B., Hignett, P., 2002. Wavelength dependence of the absorption of black carbon particles: predictions and results from the TARFOX experiment and implications for the aerosol single scattering albedo. J. Atmos. Sci. 59, 567−577.

Bibi, H., Alam, K., Bibi, S., 2016. In-depth discrimination of aerosol types using multiple clustering techniques over four locations in Indo-Gangetic plains. Atmos. Res. 181, 106−114.

Bibi, S., Alam, K., Chishtie, F., Bibi, H., 2017. Characterization of absorbing aerosol types using ground and satellites based observations over an urban environment. Atmos. Environ. 150, 126−135.

Bilal, M., Nichol, J.E. 2015. Evaluation of MODIS aerosol retrieval algorithms over the Beijing-Tianjin-Hebei region during low to very high pollution events. . Geophys. Res. Atmos.,120, doi:10.1002/2015JD023082.

Bilal, M., Nichol, J.E., Bleiweiss, M.P., Dubois, D.W. 2013. A Simplified high resolution MODIS Aerosol Retrieval Algorithm (SARA) for use over mixed surfaces. Rem. Sens. Environ. 136, 135–145.

Cazorla, A., Bahadur, R., Suski, K., Cahill, J.F., Chand, D., Schmid, B., Ramanathan, V., Prather, K., 2013. Relating aerosol absorption due to soot, organic carbon, and dust to emission sources determined from in-situ chemical measurements. Atmos. Chem. Phys. 13, 9337−9350.

Chen, Q.X., Yuan, Y., Shuai, Y., Tan, H.P., 2016. Graphical aerosol classification method using aerosol relative optical depth. Atmos. Environ. 135, 84–91.

Choi, Y.-S., Ho, C.-H., Oh, H.-R., Park, R.J., Song, C.-G., 2009. Estimating bulk optical properties of aerosols over the western North Pacific by using MODIS and CERES measurements. Atmos. Environ. 43, 5654−5660.

Dubovik, O., Holben, B.N., Eck, T.F., Smirnov, A., Kaufman,Y.J., King, M.D.,Tanre, D., Slutsker,I., 2002. Variability of absorption and optical properties of key aerosol types observed in worldwide locations. J. Atmos. Sci. 59, 590–608.

Eck, T., Holben, B.N., Reid, J., Dubovik, O., Smirnov, A., O'Neill, N., Slutsker, I., Kinne, S., 1999. Wavelength dependence of the opticaldepth of biomass burning, urban, and desert dust aerosols. J. Geophys. Res. 104(D24), 31333– 31349.

Eck, T.F., Holben, B.N., Sinyuk, A., Pinker, R., Goloub, P., Chen, H., Chatenet, B., Li, Z., Singh, R.P., Tripathi, S.N., 2010. Climatological aspects of the optical properties of fine/coarse mode aerosol mixtures. J. Geophys. Res. 115, D19205.

Farahat, A., 2016. Air pollution in the Arabian Peninsula (Saudi Arabia, the United Arab Emirates, Kuwait, Qatar, Bahrain, and Oman): Causes, effects, and aerosol categorization. Arab. J. Geosci. 9, 196.

Farahat, A., El-Askary, H., Adetokunbo, P., Fuad, A.-T., 2016. Analysis of aerosol absorption properties and transport over North Africa and the Middle East using AERONET data. Ann. Geophys., 34, 1031–1044.

Farahmandkia, Z., Mehrasbi, M.R., Sekhavatjou, M.S., 2010. Relationship between concentrations of heavy metals in wet precipitation and atmospheric PM10 particles in Zanjan, Iran. Iranian Journal of Environmental Health and Sciences Engineering, 8, 49−56.

Foroushani, M.A., Opp, C., Groll, M., 2019. Chemical Characterization of Aeolian Dust Deposition in Southern and Western Iran. Asian J. Geograph. Res. 2,1−22.

Gautam, R., Hsu, N.C., Kafatos, M., Tsay, S.-C., 2007. Influences of winter haze on fog/low cloud over the Indo-Gangetic plains. J. Geophys. Res. 112, D05207, doi:10.1029/2005JD007036.

Gerivani, H., Lashkaripour, G.R., Ghafoori, M., Jalali, N., The source of dust storm in Iran: A case study based on geological information and rainfall data. Carpathian J. Earth Environ. Sci. 2011, 6.

Gharibzadeh, M., Alam, K., Abedini, Y., Bidokhti, A.A., Masoumi, A., Bibi, H., 2018. Characterization of aerosol optical properties using multiple clustering techniques over Zanjan, Iran, during 2010-2013. Appl Opt. 57:2881−2889.

Gyawali, M., Arnott, W.P., Zaveri, R.A., Song, C., Moosmüller, H., Liu, L., Mishchenko, M.I., Chen, L.-W.A., Green, M.C.,Watson, J.G., Chow, J.C., 2012. Photoacoustic optical propertiesat UV, VIS, and near IR wavelengths for laboratory generatedand winter time ambient urban aerosols. Atmos. Chem. Phys. 12, 2587–2601.

Giles, D.M., Holben, B.N., Eck, T.F., Sinyuk, A., Smirnov, A., Slutsker, I., Dickerson, R., Thompson, A., Schafer, J., 2012. An analysis of AERONET aerosol absorption properties and classifications representative of aerosol source regions. J. Geophys. Res. 117, D17203.

Giles, D.M., Holben, B.N., Tripathi, S.N., Eck, T.F., Newcomb, W.W., Slutsker, I., Dickerson, R.R., Thompson, A.M., Mattoo, S., Wang, S.H., 2011. Aerosol properties over the Indo-Gangetic Plain: a mesoscale perspective from the TIGERZ experiment. J. Geophys. Res. 116, D18203.

Goudie, A.S., 2014. Desert dust and human health disorders. Environment International 63, 101-113.

Graaf, D.M., Stammes, P., Torres, O., Koelemeijer, R., 20
05. Absorbing aerosol index: sensitivity analysis, application to GOME and comparison with TOMS. J. Geophys. Res. 110, D01201.

Hermida, L., Merino, A., Sánchez, J.L., Fernández-González, S., García-Ortega, E., López, L., 2017. Characterization of synoptic patterns causing dust outbreaks that affect the Arabian Peninsula. Atmos. Res., 199, 29−39.

Higurashi, A., Nakajima, T., 2002. Detection of aerosol types over the East China Sea near Japan from four-channel satellite data. Geophys. Res. Lett. 29, 1836.

Holben, B.N., Eck, T., Slutsker, I., Tanre, D., Buis, J., Setzer, A., Vermote, E., Reagan, J.A., Kaufman, Y., Nakajima, T., 1998. AERONETda federated instrument network and data archive for aerosol characterization. Rem. Sens. Environ. 66, 1−16.

Hu, Z., Zhao, C., Huang, J., Leung Ruby, L., Qian, Y., Yu, H., Huang, L., Kalashnikova, O., 2016. Trans-Pacific transport and evolution of aerosols: Evaluation of quasi-global WRF-Chem simulation with multiple observations. Geosci. Model Dev. 9, 1725–1746.

Hsu, N.C., Gautam, R., Sayer, A.M., Bettenhausen, C., Li, C., Jeong, M.J., Tsay, S.-C., Holben, B.N., 2012. Global and regional trends of aerosol optical depth over land and ocean using SeaWiFS measurements from 1997 to 2010. Atmos. Chem. Phys. 12, 8037–8053.

Islam, M.N., Ali, M.A., Islam, M.M. 2019. Spatiotemporal Investigations of Aerosol Optical Properties Over Bangladesh for the Period 2002–2016. Earth Syst Environ 3, 563–573.

Jiries, A., 2003. Vehicular Contamination of Dust in Amman, Jordan. The Environmentalist 23, 205–210.

Jose, S., Niranjan, K., Gharai, B., Rao, P.V.N., Nair, V.S., 2016. Characterisation of absorbing aerosols using ground and satellite data at an urban location, Hyderabad. Aeros. Air Qual. Res. 16, 1427−1440.

Kang, J. Liu, T., Keller, J., Lin, H., 2013. Asian dust storm events are associated with an acute increase in stroke hospitalisation. J. Edipemiol. Community Health 67, 125−131.

Kang, L., Chen, S., Huang, J., Zhao, S., Ma, X., Yuan, T., Zhang, X., Xie, T., 2017. The Spatial and Temporal Distributions of Absorbing Aerosols over East Asia. Remote Sens. 9, 1050; doi:10.3390/rs9101050.

Kaskaoutis, D.G., Kambezidis, H.D., Hatzianastassiou, N., Kosmopoulos, P.G., Badarinath, K.V.S., 2007. Aerosol Climatology: On the discrimination of aerosol types over four AERONET sites. Atmos. Chem. Phys. Discuss. 7, 6357−6411.

Kaskaoutis, D.G., Kumar Kharol, S., Sinha, P.R., Singh, R.P., Kambezidis, H.D., Rani Sharma, A., Badarinath, K.V.S., 2011. Extremely large anthropogenic aerosol component over the Bay of Bengal during winter season. Atmos. Chem. Phys. 11, 7097−7117.

Kaskaoutis, D.G., Nastos, P.T., Kosmopoulos, P.G., Kambezidis, H.D., Kharol, S.K., Badarinath, K.V.S., 2010. The Aura-OMI Aerosol Index distribution over Greece. Atmos. Res, 98, 28-39.

Kaufman, Y., Boucher, O., Tanre, D., Chin, M., Remer, L., Takemura, T., 2005. Aerosol anthropogenic component estimated from satellite data. Geophys. Res. Lett. 32, L17804. http://dx.doi.org/10.1029/2005GL023125.

Kedia, S., Ramachandran, S., Holben, B.N., Tripathi, S., 2014. Quantification of aerosol type, and sources of aerosols over the Indo-Gangetic Plain. Atmos. Environ. 98, 607−619.

Khaniabadi, Y.O., Daryanoosh, S.M., Amrane, A., Polosa, R., Hopke, P.K. et al.. 2017. Impact of Middle Eastern Dust storms on human health. Atmos. Poll. Res. 8, 606−613.

Kim, D., Chin, M., Bian, H., Tan, Q., Brown, M.E., Zheng, T., You, R., Diehl, T., Ginoux, P., Kucsera, T., 2013. The effect of the dynamic surface bareness on dust source function, emission, and distribution, J. Geophys. Res. 118, 1–16.

Kumar, K.R., Attada, R., Dasari, H.P., Vellore, R.K., Langdon, S., Abualnaja,Y.O., Hoteit, I., 2018. Aerosol Optical Depth variability over the Arabian Peninsula as inferred from satellite measurements. Atmos. Environ. 187, 346−357.

Lee, K., Chung, C., 2012. Observationally-constrained estimates of global small mode AOD. Atmos. Chem. Phys. Discuss. 12, 31663−31698.

Lee, J., Kim, J., Song, C., Kim, S., Chun, Y., Sohn, B., Holben, B.N., 2010. Characteristics of aerosol types from AERONET sunphotometer measurements. Atmos. Environ. 44, 3110−3117.

Leili, M., Naddafi, K., Nabizadeh, R., Yunesian, M., Mesdaghinia, A., 2008. The study of TSP and PM10 concentration and their heavy metal content in central area of Tehran, Iran. Air Qual Atmos Health 1, 159–166.

Levelt, P.F., Hilsenrath, E., Leppelmeier, G.W., van den Oord, G.H., Bhartia, P.K., Tamminen, J., de Haan, J.F., Veefkind, J.P., 2006. Science objectives of the ozone monitoring instrument. IEEE Geosci. Remote Sens. Lett. 44, 1199−1208.

Li, J., Liu, C., Yin, Y., Kumar, K.R., 2016. Numerical investigationon the Ångström Exponent of black carbon aerosols. J. Geophys.Res. 121, 3506–3518.

Logan, T., Xi, B., Dong, X., Li, Z., Cribb, M., 2013. Classification and investigation of Asian aerosol absorptive properties. Atmos. Chem. Phys. 13, 2253−2265.

Logothetis, S.-A., Salamalikis, V., Kazantzidis, A., 2020. Aerosol classification in Europe, Middle East, North Africa and Arabian Peninsula based on AERONET Version 3. Atmos. Res., 239, 104893.

Mashat, A.W.S., Awad, A.M., Alamoudi, A.M., Assiri, M.E., 2019. Monthly and seasonal variability of dust events over northern Saudi Arabia. Int. J. Climatol. 2019, 1–23.

Mashat, A.W.S., Awad, A.M., Assiri, M.E., Labban, A.H., 2020. Dynamic and synoptic study of spring dust storms over northern Saudi Arabia. Theor. Appl. Climatol. 140, 619–634.

Omar, A.H., Won, J.-G., Winker, D.M., Yoon, S.-C., Dubovik, O., McCormick, M.P., 2005. Development of global aerosol models using cluster analysis of Aerosol Robotic Network (AERONET) measurements. J. Geophys. Res., 110, D10S14.

Omar, A.H., Winker, D.M., Vaughan, M.A., Hu, Y., Trepte, C.R., Ferrare, R.A., Lee, K.P., Hostetler, C.A., Kittaka, C., Rogers, R.R., Kuehn, R.E., 2009. The CALIPSO Automated Aerosol Classification and Lidar Ratio Selection Algorithm. J. Atmos. Ocean. Tech. 26, 1994–2014.

Onishi, K. Otani, S., Yoshida, A., Mu, H., Kurozawa, Y., 2012. Adverse Health Effects of Asian Dust Particles and Heavy Metals in Japan. Asia-Pacific Journal of Public Health Asia Pac J Public Health 27, NP1719-26.

Pérez-Ramírez, D., Veselovskii, I., Whiteman, D.N., Suvorina, A., Korenskiy, M., et al., 2015. High temporal resolution estimates of columnar aerosol microphysical parameters from spectrum of aerosol optical depth by linear estimation: application to long-term AERONET and star-photometry measurements. Atmos. Meas. Tech. 8, 3117–3133.

Prakash, P.J., Stenchikov, G., Kalenderski, S., Osipov, S., Bangalath, H., 2015. The impact of dust storms on the Arabian Peninsula and the Red Sea. Atmos. Chem. Phys. 15, 199–222.

Prospero, J.M., Ginoux, P., Torres, O., Nicholson, S.E., Thomas, E.G., 2002. Environmental characterization of global sources of atmospheric soil dust identified with Nimbus 7 total ozone mapping spectrometer (TOMS) absorbing aerosol product. Rev. Geophys. 40: 2–31.

Ram, K., Singh, S., Sarin, M., Srivastava, A., Tripathi, S., 2016. Variability in aerosol optical properties over an urban site, Kanpur, in the Indo-Gangetic Plain: a case study of haze and dust events. Atmos. Res. 174, 52−61.

Rupakheti, D., Kang, S., Bilal, M., Gong, J., Xia, X., Cong, Z., 2019. Aerosol optical depth climatology over Central Asian countries based on Aqua-MODIS Collection 6.1 data: Aerosol variations and sources. Atmos. Environ. 207, 205–214.

Rupakheti, D., Kang, S., Rupakheti, M., Cong, Z., Panday, A.K., Holben, B.N., 2019a. Identification of absorbing aerosol types at a site in the northern edge of Indo-Gangetic Plain and a polluted valley in the foothills of the central Himalayas. Atmos. Res. 223, 15-23.

Russell, P., Bergstrom, R., Shinozuka, Y., Clarke, A., DeCarlo, P., Jimenez, J.,Livingston, J., Redemann, J., Dubovik, O., Strawa, A., 2010. Absorption Ångström Exponent in AERONET and related data as an indicator of aerosol composition. Atmos. Chem. Phys. 10, 1155−1169.

Sabbah, I., Hasan, F.M., 2008. Remote sensing of aerosols over the Solar Village, Saudi Arabia. Atmos. Res. 90, 170–179.

Saeedi, M. Li, L.Y., Salmanzadeh, M., 2012. Heavy metals and polycyclic aromatic hydrocarbons: Pollution and ecological risk assessment in street dust of Tehran. Journal of Hazardous Materials 227–228, 9–17.

Schmeisser, L., Andrews, E., Ogren, J. A., Sheridan, P., Jefferson, A., et al., 2017. Classifying aerosol type using in situ surface spectral aerosol optical properties. Atmos. Chem. Phys. 17, 12097−12120.

Shao, Y., 2008. Physics and Modelling of Wind Erosion, Springer, Berlin, Germany.

Shen, X., Bilal, M., Qiu, Z., Sun, D., Wang, S., Zhu, W., 2019. Long-term spatiotemporal variations of aerosol optical depth over Yellow and Bohai Sea. Environ. Sci. Poll. Res. 26, 7969–7979.

Shin, S.K., Tesche, M., Noh, Y., Müller, D. 2019. Aerosol-type classification based on AERONET version 3 inversion products. Atmos. Meas. Tech., 12, 3789–3803.

Shin, S.K., Tesche, M., Müller, D., Noh, Y. 2019. Technical note: Absorption aerosol optical depth components from AERONET observations of mixed dust plumes. Atmos. Meas. Tech., 12, 607–618.

Srivastava, A. K., S. N. Tripathi, S. Dey, V. P. Kanawade, S. Tiwari, 2012. Inferring aerosol types over the Indo-Gangetic Basin from ground based sunphotometer measurements. Atmos. Res. 109–110, 64–75.

Su, B., Li, H., Zhang, M., Bilal, M., Wang, M., Atique, L., Zhang, Z., Zhang, C., Han, G., Qiu, Z., Ali, M.A. 2020. Optical and Physical Characteristics of Aerosol Vertical Layers over Northeastern China. Atmosphere, 11, 501.

Tiwari, S., Srivastava, A.K., Singh, A.K., Singh, S., 2015. Identification of aerosol types over Indo-Gangetic Basin: implications to optical properties and associated radiative forcing. Environ. Sci. Poll. Res. 22, 12246–12260.

Torres, O., Chen, Z., Ahn, C., 2009. Aerosol absorption measurements from space by the Aura-OMI sensor. In: Proc. STAR Science Seminar, NOAA-NESDIS, Camp Springs, MD. https://www.star.nesdis.noaa.gov/star/documents/seminardocs/Torres_20090702.pdf.

Torres, O., Tanskanen, A., Veihelmann, B., Ahn, C., Braak, R., Bhartia, P.K., Veefkind, P., Levelt, P., 2007. Aerosols and surface UV products from Ozone Monitoring Instrument observations: an overview. J. Geophys. Res. 112, D24S47.

Wang, S., Fang, L., Gu, X., Yu, T., Gao, J., 2011. Comparison of aerosol optical properties from Beijing and Kanpur. Atmos. Environ. 45, 7406−7414.

Wilks, D.S., 2006. Statistical Methods in the Atmospheric Sciences, Academic Press, Amsterdam Boston, Heidelberg, London.

Williams, J.B., Shobrak, M., Wilms, T.M., Arif, I.A., Khan, H.A., 2012. Climate change and animals in Saudi Arabia. Saudi Journal of Biological Sciences 19, 121–130.

Winker, D.M., Pelon, J.R., McCormick, M.P., 2003. The CALIPSO mission: spaceborne lidar for observation of aerosols and clouds. In: Third International Asia-Pacific Environmental Remote Sensing of the Atmosphere, Ocean, Environment, and Space. International Society for Optics and Photonics,pp. 1e11. Proc. SPIE 4893.

Wu, Y.L., Li, H.W., Chien, C.H., Lai, Y.C., Wang, L.C., 2010. Monitoring and Identification of Polychlorinated Dibenzo-p-dioxins and Dibenzofurans in the Ambient Central Taiwan. Aeros. Air Qual. Res. 10, 463–471.

Wu, Y., Zhu, J., Che, H., Xia, X., Zhang, R., 2015. Column-integrated aerosol optical properties and direct radiative forcing based on sun photometer measurements at a semi-arid rural site in Northeast China. Atmos. Res. 157, 56–65.

Yu, Y., Notaro, M., Liu, Z., Kalashnikova, O., Alkolibi, F., Fadda, E., Bakhrjy, F., 2013. Assessing temporal and spatial variations in atmospheric dust over Saudi Arabia through satellite, radiometric, and station data. J. Geophys. Res. Atmos. 118, 13253–13264.

Highlights

- AERONET, OMI, and CALIPSO datasets were used for classifying aerosols
- OMI AAOD shows the dominance of absorbing aerosols with high seasonal variability
- Dust, then mixed black carbon and dust dominated over the study area, Saudi Arabia
- Mixed aerosol types suggest increasing fossil fuel and biogenic emissions
- FMF vs. (AE, AAE, and SSA) are the best techniques for classifying aerosols